NAVAL UNDERWATER SYSTEMS CENTER
NEW LONDON LABORATORY
NEW LONDON, CONNECTICUT   06320

Technical Memorandum

APPLICATION OF LINEAR PREDICTIVE SPECTRAL ANALYSIS
TO MULTIPLE TONES IN NOISE

DATE: 12 December 1979

Author: _Albert H Nuttall_
ALBERT H. NUTTALL
Special Projects Dept.
Advanced Systems
Technology Division

20030930 062

ABSTRACT

An application of linear predictive spectral analysis, in particular the forward-and-backward averaging procedure, to tones in noise is made. The accurate tone-frequency estimation capability and lack of tone-splitting make this an attractive technique for spectral analysis and estimation of tone amplitudes. The effect of inadequate pole-order on the spectral estimate in white and colored noise is investigated in a number of examples. The examples here indicate that the linear predictive technique should receive wider application for spectral analysis in the realm of underwater acoustics. Two programs in BASIC for the Hewlett Packard 9845 for the cases of real and complex data have been written and are available from the author; they are modifications to the original program in FORTRAN written by S.L. Marple.

ADMINISTRATIVE INFORMATION

3/4

INTRODUCTION

The linear predictive technique of spectral analysis has received a great deal of attention lately; see refs. 1 and 2 and the references listed therein. A comparison of several linear predictive techniques was made in ref. 3, with the conclusion that the then newly-proposed forward-and-backward (F&B) averaging technique and the Burg technique (ref. 4) were as good as any currently available. The reason that the Burg technique has been preferred over the F&B technique is not due to the quality of the spectral estimate (see ref. 3, page 81), but mainly that a recursive procedure exists for the solution of the matrix equations for the Burg technique, whereas a full-order matrix inversion was required for the F&B technique at each filter-order considered. The fact that the F&B technique can occasionally (rarely) yield an unstable correlation recursion or a spiky spectral estimate (ref. 3, pages 41 and 35), is not a severe limitation of the technique in practice; in fact, for data sets of 100 points or more, this author has not yet seen any examples of poles outside the unit circle in the z-plane, although some have come extremely close.

A recent contribution by Marple, ref. 5, has now altered the computational situation considerably. Specifically, he has derived a recursive algorithm for the solution of the matrix equations of the F&B technique, where the number of computations are comparable to that required for the Burg technique. Furthermore, he has shown that the F&B technique is not subject to line-splitting (ref. 6), as the Burg technique is, nor are the spectral peaks as biased when estimating the tone frequency location. The reason for these desirable features is that the F&B technique is an unconstrained p-th order least squares minimization, whereas the Burg

technique is a constrained progressive-minimization procedure, structured so as to satisfy a preconceived recursive algorithm (ref. 3, sections 4.6 and 4.7).

Accordingly, it is now reasonable and well-advised to reconsider the F&B linear predictive technique for spectral analysis of typical underwater acoustic waveforms which can include several tones of widely different levels in colored noise. In view of the "global" optimization property (ref. 1, page 572) of the linear predictive technique, such high dynamic-range spectra should not be too adverse cases for consideration. This memorandum will consider several such examples and point out some important features and properties of the linear predictive F&B technique.

POWER CONTRIBUTION FROM ONE POLE-PAIR

The power density spectral estimate of the linear predictive technique takes the form, at p-th order, of (ref. 1, page 568)

$$P(f) = \frac{\Delta E}{\left| \sum_{k=0}^{p} a_k \exp(-i 2\pi f k \Delta) \right|^2} = \frac{\Delta E}{\left| a\left(\exp(i 2\pi f \Delta) \right) \right|^2}, \quad |f| < \frac{1}{2\Delta}, \quad (1)$$

where polynomial

$$a(z) \equiv \sum_{k=0}^{p} a_k z^{-k}, \quad (2)$$

Δ is the time-sampling increment, E is the prediction-error power at p-th order, $a_0 = 1$, and $\{a_k\}_1^p$ are the p-th order prediction-filter coefficients. Generalizing (1) to the complex z-plane, and allowing for complex data and filters, we express (1) as

$$P(z) = \frac{\Delta E}{a(z) \, a^*(1/z^*)}, \quad (3)$$

meaning that the spectral estimate in (1) is given by

$$P\left(\exp(i 2\pi f \Delta) \right) = P(f). \quad (4)$$

Now if $a(z)$ has a zero at z_0, which is near the unit circle in the z-plane, then $P(z)$ has a pole-pair at the points z_0, $1/z_0^*$, which are both close to the unit circle and located on the same radius vector; see figure 1. This gives rise to a
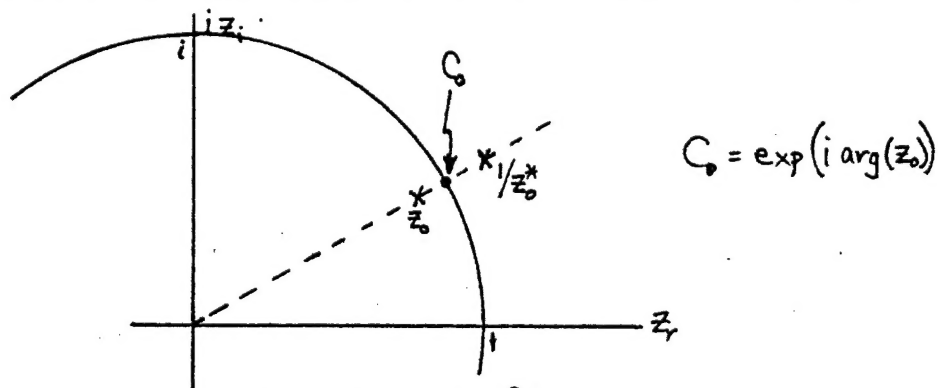

Figure 1. One Pole-Pair of $P(z)$

7

peak in the spectral function P(f), near the frequency

$$f_0 \equiv \frac{1}{2\Delta} \frac{arg(z_0)}{\pi} = f_N \frac{arg(z_0)}{\pi} ,$$ (5)

where $f_N = (2\Delta)^{-1}$ is the Nyquist frequency. And if $|z_0| \approx 1$, the spectral peak is very large and narrow, with 3 dB bandwidth B approximately equal to

$$B = \frac{2(1-|z|)}{\pi} \frac{1}{2\Delta} = \frac{2(1-|z_0|)}{\pi} f_N .$$ (6)

If the values of f, at which P(f) is calculated, have an increment larger than bandwidth (6), the peak of this spectral component can be missed, and a misleading spectral calculation can result. One way to alleviate this situation is to calculate the power contribution due to the pole-pair in figure 1, and output this information in addition to calculated values of the spectral estimate. We evaluate this power as follows: express (3) as

$$P(z) \equiv \frac{R(z)}{(z-z_0)(z^{-1}-z_0^*)} \cong \frac{R(C_0)}{(z-z_0)(z^{-1}-z_0^*)} \equiv P_a(z)$$ (7)

for z near z_0; see figure 1. The approximation to the spectrum in the neighborhood of C_0 in figure 1 is

$$P_a\left(\exp(i2\pi f\Delta)\right) = \frac{R(C_0)}{\left|\exp(i2\pi f\Delta)-z_0\right|^2} .$$ (8)

The area under this approximation is called the power contribution of the pole-pair corresponding to z_0, and is given by the integral over the entire frequency interval:

$$P_0 \equiv \int_{-1/2\Delta}^{1/2\Delta} df \ P_a\left(\exp(i2\pi f\Delta)\right) = \frac{1}{i2\pi\Delta} \oint \frac{dz}{z} P_a(z)$$

$$= \frac{1}{i2\pi\Delta} \oint dz \frac{R(C_0)}{(z-z_0)(1-zz_0^*)} = \frac{1}{\Delta} \frac{R(C_0)}{1-|z_0|^2} ,$$ (9)

where $\oint$ denotes counter-clockwise integration around the unit circle in the z-plane. (Result (9) presumes $|z_0| < 1$; if $|z_0| > 1$, we get $\frac{1}{\Delta} R(C_0)/(|z_0|^2-1)$).

Now we eliminate unknown $R(c_0)$ from (9), by observing from (7) that

$$P(c_0) = \frac{R(c_0)}{(c_0 - z_0)(c_0^* - z_0^*)} = \frac{R(c_0)}{(1 - |z_0|)^2} \,. \tag{10}$$

Then (9), (3), (2), and (5) yield for the pole-power

$$P_0 = \frac{P(c_0)}{\Delta} \frac{1 - |z_0|}{1 + |z_0|} = \frac{E}{\left| \sum_k a_k c_0^{-k} \right|^2} \frac{1 - |z_0|}{1 + |z_0|}$$

$$= \frac{E}{\left| \sum_k a_k \exp(-i 2\pi f_0 \Delta k) \right|^2} \frac{1 - |z_0|}{1 + |z_0|} \,. \tag{11}$$

This calculation requires that one evaluate both the magnitude and argument of the pole location z_0 of $P(z)$ under investigation, since

$$c_0 = \exp(i 2\pi f_0 \Delta) = \exp(i \arg(z_0)). \tag{12}$$

Recall that $\{a_k\}$ are the filter coefficients, and E is the prediction-error power, all quantities evaluated for p-th order. Alternatively, z_0 is a zero location of $a(z)$ defined in (2).

For a real process, pole-pairs of $P(z)$ occur in conjugate symmetry, and the spectrum P(f), given by (4), is even about $f=0$. It is then convenient to plot only positive frequencies, from 0 to f_N, and double the results above. Then we have for the pole-power contribution

$$P_0 (\text{real data}) = \frac{2E}{\left| \sum_k a_k \exp(-i 2\pi f_0 \Delta k) \right|^2} \frac{1 - |z_0|}{1 + |z_0|} \,. \tag{13}$$

The 3-dB bandwidth is unchanged from (6), however.

9

VOLTAGE AMPLITUDE OF A POLE-PAIR

Although the pole locations of $P(z)$ in (3) give a good indication of the frequencies of pure tones, the estimated power contributions due to these poles are not always good indicators of the amplitudes of pure tones, because a slight radial movement of a pole near the unit circle causes a large change in the estimated power contribution; see (11). This becomes a very pronounced effect for tones with a large SNR (signal-to-noise ratio), a condition where we should expect better indicators rather than poorer ones. Therefore, an alternative technique to using the pole-power contribution is preferred.

Since we have a good estimate f_0 of a tone frequency from (5), we can estimate the corresponding tone amplitude according to

$$\frac{1}{N} \left| \sum_{n=1}^{N} X_n \exp\left(-i 2\pi f_0 \Delta n\right) \right| , \tag{14}$$

where $\{X_n\}_1^N$ is the available data. (For real data, we must take 2 times this result). As a refinement, we could perturb f_0 slightly, to find the local maximum of this function. This has been found to be a good technique in practice, for high SNR tones. It gives a low-amplitude indication for spectral peaks due to spurious poles, and a high-amplitude indication for strong tones that are actually present. We needn't perform a fine-grained search over all frequencies, because we simply choose frequency f_0 according to (5). Of course, we have to solve for the corresponding zero z_0 of $Q(z)$; however, a recursive procedure is described for this zero location in appendix A.

LINEAR PREDICTION OF TONES

We will concentrate here on multiple tones *sans* noise. Anticipation of good approximations, via linear predictive techniques applied to tones, can be justified by consideration of the following. Let complex waveform x(t) be composed of K complex exponentials of arbitrary amplitudes, frequencies, and phases, but no additive noise:

$$x(t) = \sum_{k=1}^{K} A_k \exp\left(i\, 2\pi f_k t + i\theta_k\right).$$ (15)

Then data value

$$X_n \equiv x(n\Delta) = \sum_{k=1}^{K} A_k \exp\left(i\, 2\pi f_k \Delta n + i\theta_k\right) \equiv \sum_{k=1}^{K} g_k(n).$$ (16)

It follows that

$$X_{n-1} = \sum_{k=1}^{K} \exp\left(-i\, 2\pi f_k \Delta\right) g_k(n)$$

$$\vdots$$

$$X_{n-K} = \sum_{k=1}^{K} \exp\left(-i\, 2\pi f_k \Delta K\right) g_k(n).$$ (17)

Now these K linear equations can be solved for $g_k(n)$, $1 \le k \le K$, and the results substituted in (16). The end result is an exact expression for data value x_n in terms of past data values according to

$$X_n = \sum_{k=1}^{K} a_k X_{n-k} ,$$ (18)

where coefficients $\{a_k\}$ involve $\exp\left(-i\, 2\pi f_k \Delta m\right)$, $1 \le k, m \le K$. That is, X_n can be perfectly linearly-predicted in terms of its past K data values, when there is no additive noise. Thus pure tones are good candidates for a linear predictive approach. Of course, since X_{n-K} can be expressed in terms of $X_{n-K+1}, \ldots, X_n$, from

11

(18), it also means that backward prediction is perfect, in the absence of noise.

As examples, we have the following:

for K=1,

$$X_n = e_1 X_{n-1} \; , \quad X_n = e_1^* X_{n+1} \; ; \tag{19}$$

for K=2,

$$X_n = (e_1 + e_2) X_{n-1} - (e_1 e_2) X_{n-2} \; ,$$
$$X_n = (e_1 + e_2)^* X_{n+1} - (e_1 e_2)^* X_{n+2} \; ; \tag{20}$$

for K=3,

$$X_n = (e_1 + e_2 + e_3) X_{n-1} - (e_1 e_2 + e_2 e_3 + e_3 e_1) X_{n-2} + (e_1 e_2 e_3) X_{n-3} \; ; \tag{21}$$

where

$$e_K \equiv \exp(i 2\pi f_K \Delta). \tag{22}$$

The general pattern for any K is now obvious from (19)-(21).

It should be pointed out that if a dc component is present in the data, this corresponds to one of the $f_k = 0$. Alternatively, if a process contains no dc component, but we subtract its (non-zero) sample mean, we are creating a dc component in the process, thereby requiring one-larger order for perfect prediction. This behavior is illustrated in appendix B.

EXAMPLES

Our first example is five equal-amplitude complex exponentials in no noise. As shown in (16)-(18), perfect prediction is possible with a $p=$5th order filter, (except for calculator roundoff). We selected frequencies

$$\frac{f}{f_N} = -.65, -.38, .22, .70, .85. \tag{23}$$

The results of the spectral analysis procedure* for N= 100 complex data points and a 1024-point FFT over the ±Nyquist frequency band are given in dB in figure 2 for p = 5. All the plots are normalized so that their peak value reaches the top of the 70dB range plotted. The magnitudes and arguments of the 5 zero locations of $a(z)$ are given in table 1.

Magnitude	Argument $/\pi = \hat{f}/f_N$
.999714	-.649911
.999822	-.379931
.999916	.220052
.999105	.699925
.999013	.850057

Table 1. Zero Locations of $a(z)$ for Five Tones; p = 5.

It will be observed that all zeros lie just inside the unit circle, rather than on it, and that the frequency estimate associated with each zero is accurate, but not perfect. This is due to the subtraction of the sample mean; see appendix B. The spectral amplitudes depicted in figure 2 differ amongst themselves by 12 dB, even though the true tone amplitudes were equal; there are two reasons for

---

*The sample mean was subtracted from the data set; see appendix B for a discussion of this effect. All of the results to follow also correspond to subtraction of sample mean.

this. One is that the spectral function P(f) in (1) was calculated at only 1024
points in the $\pm$Nyquist frequency range, and therefore the very narrow widths of
the peaks in P(f) have not been adequately sampled. In fact, the 3-dB bandwidths,
B/f_N, of the 5 peaks in figure 2 are, from (6), $(1.82, 1.13, 0.54, 5.70, 6.29)10^{-4}$
respectively, which are smaller than the frequency sampling increment $2/1024 =$
20×10^{-4}. This frequency sampling computation effect will contribute greatly to
the apparent fluctuation in peak spectral indication, and can be alleviated by
taking larger-size FFTs, or by calculating P(f) more finely just in the neighbor-
hood of the peak indication.

The second reason is that the peaks of P(f) do not necessarily have to
reflect true tone powers; rather it is the area under each peak which is indicative
of that tone power; see ref. 7 . A calculation of these pole-powers according to
(11) yields values .971, .967, .945, .999, and .994 respectively, compared with
the exact value of 1. The tone amplitudes, as calculated according to (14), are
.970, .980, .980, .981, and .971 respectively, instead of 1. Perturbation of f_o
in (14), about the value (5), did not significantly change the peak of (14).

When the order of the predictive filter is taken to be p=4, instead of the
correct value of 5 for this complex data example, the results are as indicated in
figure 3. The two closest tones at .7 and .85 are not resolved. The pole-powers
are given as .99, 1.24, 1.03, and 1.85 respectively, indicating a lumping together
of the two closest tones. The tonal amplitudes are grossly in error since none
of the 5 frequencies were estimated accurately enough. This example points out
the deleterious effect of too low an order, p, for the predictive filter.

Our next example consists of the same five complex exponentials with white noise added, to yield a signal-to-noise power ratio (SNR)[*] of 7.8 dB per tone, as measured in the Nyquist frequency interval $\left(-f_N, f_N\right)$. First, in figure 4 is presented the spectral plot for a fifth-order prediction filter, p=5. The frequency estimates according to (5) are in error by $\left|f/f_N\right|$ =.004, on the average. The pole-powers and tone amplitudes are 1.06, 1.10, 1.01, .93, 1.22 and .97, .88, .96, .67, 1.02 respectively.

When we repeat this same example with p changed to 10, the situation is much improved, as figure 5 indicates. The frequency estimates are now in error by $\left|f/f_N\right|$ =.0007, on the average. The pole-powers and tone amplitudes are 1.05, .83, 1.00, .76, 1.30 and 1.00, 1.04, .99, .92, 1.02 respectively. We notice a significant improvement in amplitude estimation, which is due mainly to the improved frequency estimates. The pole-powers are more erratic than for figure 4.

When the SNR per tone is reduced further, to 0 dB as measured in the Nyquist band, the results in figures 6 and 7 are obtained for p=10 and 15 respectively. The pole-powers vary significantly from the true values for both examples; however, the tonal amplitude estimates for p=15 in figure 7 are rather good: 1.04, 1.11, 1.01, .85, 1.08. The frequency estimates are better for p=15, being in error by $\left|f/f_N\right|$ = .00073 on the average. These results are comparable to the higher SNR results in figure 5 where p=10 was used. When p is changed to 25, results substantially equivalent to figure 7 were obtained, except that there were proportionally more peaks and sharper tonal indications; see figure 8. The large variation in peak values (21dB) is not too significant when we recall the frequency sampling and tone-power considerations discussed earlier.

[*] The SNR of each tone is the ratio of each tone power to the total noise power, σ_n^2, in the Nyquist band $\left(-f_N, f_N\right)$.

We now consider a case of N=1000 <u>real</u> data points with 9 tones of unequal

value in white noise. Specifically, the tonal amplitudes, powers, and frequencies

are listed in table 2. Spectral analysis results are presented in figures 9-11,

Amplitude	Power	Frequency/Nyquist
1	0.5	.11
5	12.5	.19
2	2.0	.32
8	32.0	.41
3	4.5	.53
6	18.0	.62
1	0.5	.69
7	24.5	.77
5	12.5	.89

Table 2.   Nine-Tone Example

for p=18, 20, and 25, respectively for noise power $\sigma_n^2 = \frac{1}{12}$. Due to the realness of

the data, we only need plot   the even spectrum from 0 to f_N. Figure 9, for

p=18, barely gives any indication of the weak tone at f/f_N =.69, despite the fact

that 9 real tones can be predicted via an 18 pole filter if noise were absent.

Increasing p to 20 or 25 clearly indicates all 9 tones. The relative peaks in

figures 9-11 are not important, for reasons already discussed. In table 3 are given

the estimated tonal amplitudes, powers, and frequencies. For all tones, the frequency

p=20				p=25		
Amplitude	Power	Frequency/Nyquist		Amplitude	Power	Frequency/Nyquist
0.9944	0.524	.109834		0.9952	0.493	.109844
4.9931	11.324	.190012		4.9933	15.868	.190006
1.9844	1.983	.319871		1.9903	2.102	.319906
8.0100	33.175	.410001		8.0100	67.474	.410001
3.0033	4.691	.529956		3.0034	4.015	.529996
5.9866	18.917	.619992		5.9869	13.091	.619997
0.9352	0.495	.690411		0.9818	0.469	.690132
6.9967	23.956	.770020		6.9961	18.266	.770008
4.9837	14.663	.890013		4.9849	18.692	.890005

Table 3.   Estimated Parameters for Nine Tones

and amplitude estimates are better for p=25 than for p=20; however, the pole power

estimates are significantly better for p=20 than for p=25. This appears to be due to

the sensitivity of the pole-power to the proximity of the pole to the unit circle;

see (11) or (13). In fact, the best pole-power estimates for this example were

obtained at p=18. Thus there appears to be a trade-off between the pole-power and

amplitude approaches, depending on the proximity of each pole to the unit circle.

When white noise power σ_n^2 is increased to 1, the value of p must be increased

to maintain reliable results; an example is presented in figure 12. And when the

noise power is increased to 10, the spectral estimate for p=50 is given in figure 13.

The weaker tones at f/f_N = .11 and .69, which have SNRs = -13 dB, have erratic esti-

mates for their pole-powers and amplitudes. Larger values of p could conceivably

be advantageous for these lower SNR tones. Since the number of available data points

is N=1000 here, larger values of p are certainly admissable; in fact, Akaike is

quoted (ref. 1, page 575, footnote) as allowing p as large as $3N^{\frac{1}{2}}$, which would be

about 100 for this example of N=1000. The stronger tones in figures 12 and 13 still

yield reliable frequency and amplitude estimates. For example, in figure 13, 1 dB

tone at f/f_N = .19 is estimated to be at .1901, with amplitude 4.91 (rather than 5),

and the pole-power estimate is 11.2 (rather than 12.5). Similarly, the equal-

strength tone at f/f_N = .89 is estimated to be at .8902, with amplitude 4.69. The

correspondings estimates for the larger SNR case in figure 12 were even better.

We now consider some examples of tones in colored noise. In particular, the

additive-noise spectrum is depicted in figure 14 and is observed to have a 45 dB

dynamic range over the zero-to-Nyquist frequency interval; see appendix C for this noise

example. We now add three tones at the frequencies

$$f = .15 f_N, \ .45 f_N, \ .65 f_N \equiv f_1, f_2, f_3, \tag{24}$$

17

with SNRs -10, -20, -30 dB respectively, where these signal-to-noise ratios are measured with respect to the noise in the entire zero-to-Nyquist band. The strongest tone at f_1 is located in the region of highest noise density. In fact, although the signal strength drops by 10 dB in going from frequency f_1 to f_2, the noise density drops by 21 dB; thus the "local" SNR (ratio of spectral densities) is better by 11 dB at f_2 relative to f_1. In going from f_2 to f_3, the signal strength drops by another 10 dB, while the noise density drops by 7 dB; thus the "local" SNR at f_2 is 3 dB better than that at f_3. A more thorough treatment is given in appendix C.

The spectral estimate for N=1000 and p=25 is shown in figure 15. As anticipated by the "local" SNR results above, the sharpest and most accurate spectral peak is near f_2. The frequency corresponding to the argument of the pole-pair is written directly above each peak in figure 15 et seq., thereby enabling a ready measure of accuracy.

In figures 16 and 17, the data is left unchanged, and p is increased to 50 and 75, respectively. The frequency estimates are progressively better in figures 15-17. The tone amplitude estimates in figure 17 for p=75 are accurate within 1.2%, 2.3%, and .02% respectively, of the true values; the pole-powers are less accurate, being off by 16%, 16.3% and 1.7%, respectively.

In the next series of plots, the tones are decreased 10 dB in strength, to -20, -30, -40 dB SNR at f_1, f_2, f_3, respectively. Figures 18-21 correspond respectively to p=75, 100, 125, 150.

The two weaker tones, of -30 dB SNR at $f/f_N = .45$, and -40 dB SNR at $f/f_N = .65$, are both very well indicated for all the values of p considered; however the strongest tone, of -20 dB SNR at $f/f_N = .15$, is never really indicated at all. The

only reason we indicated the frequency corresponding to the argument of the pole near f/f_N = .15, is that we knew the true tone location for this simulation example. In practice, the spectral peak at f/f_N = .15 is not significantly larger than its neighbors to be able to declare it reliably; in fact, the spurious peak near f/f_N = .54 is larger than the true tone at f/f_N = .15. This example points out that the "local" SNR (ratio of signal energy to noise spectral density) is more important in detecting and estimating tones that the "global" SNR (ratio of tone power to noise power). This result is similar to the standard FFT approach. Also see appendix C.

The "ribbon width" of fluctuations, in the spectral estimates of figures 18-21, is uniform with frequency, regardless of the local density value; see ref. 1, page 572. However, this ribbon width is increasing as the order, p, of the filter increases. This is a manifestation of the resolution-vs.-stability tradeoff that one must accept in spectral analysis. Specifically, as p increases, the frequency resolution improves, but the stability of the estimates degrades.

The relative amplitudes of the tone indications near f/f_N = .45 and .65 in figures 18-21 are not important, because these peaks are narrower than the FFT frequency-increment, and we undoubtedly missed the maximum peak value; for example, in figure 21, the 3 dB bandwidth of the peak near f/f_N = .65 is .001 whereas the frequency increment is 2/1024 = .002. Thus, since the pole shifts slightly when p is changed, we can get variable spectral indications. The tone amplitude indicators are rather good for figure 21, being in error by 2.1%, 8.3%, and 5.6% respectively.

The frequency accuracy of the two weaker tones is extremely good, despite the low SNR. The minimum error is realized for p=125 for this particular example.

The best value of p to use probably depends on N, the number of data points available, and the local SNR. Whether the number of tones present is a factor is unknown.

One last example of eight tones with various SNRs ranging from -10 dB to -50 dB is presented in figures 22 and 23 for p=150 and 200, respectively. The frequency and SNR of each tone is indicated under the peak indication, while the estimated frequency is written above the peak, in figure 22. The two tones corresponding to f/f_N = .15 and .75 are not detectable; on the other hand, the -50 dB SNR tone at .95 is clearly detectable. Increasing p to 200 in figure 23 gives a rather clear indication of the tone at .15, but the tone at .07 is marginal now; but in neither case is the tone at .75 detected.*

When the strength of the tone at f/f_N = .75 was increased by 10 dB, its spectral indication increased by 20 dB. This indicates a thresholding effect; that is, if the local SNR is sufficiently large, a good indication of tone presence is obtained, but if the SNR is decreased, this indication rapidly disappears.*

---

* In appendix C, a quantitative measure of detectability is defined and illustrated for this example of eight tones.

COMMENTS

The applicability of linear predictive spectral analysis to multiple tones in noise has been demonstrated in a number of examples, including some tones with very small SNR. The best filter-order, p, to choose depends on the number of available data points, N, and is also probably a function of the local SNR (ratio of signal energy to noise density) at the frequency of interest. What may be indicated here is several plots, each for a different value of p, all computed from the same data, in order to best detect and estimate different level tones in colored background noise. If so, the recursive procedure of ref. 5 is very useful, since one can plot spectral estimates at any selected points of the recursion.

If only one large value of p is of interest, an apparent alternative procedure is to use the straightforward matrix inverse approach for that order p alone. This may be quicker and more accurate, if the computational effort is smaller. However, a pxp matrix will be necessary to store the sample correlations required in the F&B technique, and this can be excessive for large p ($>$100). The storage requirements of the Marple algorithm are very reasonable, even for very large p. Nevertheless, it would be worthwhile to conduct at least one data set through both procedures, in order to ascertain the accuracy and reliability of these extensive data-processing routines that are being contemplated.

Some results on a comparison of linear predictive techniques with conventional Fourier analysis, and resolution capabilities of each, are presented in refs. 8 and 9.

PROGRAMS

A Fortran program for the recursive solution of the predictive-filter coefficients, via the normal matrix equations encountered in the linear predictive F&B technique, has been presented in ref. 5. This program has been modified some-what here and written in BASIC for the Hewlett Packard 9845 Calculator, for the two cases of real data and complex data. Modifications, leading to minimization of execution time, include: elimination of divisions in favor of multiplications; use of auxiliary variables to minimize the number of repeated calculations and table look-ups; movement of some variables outside loops to minimize look-ups; eliminate some unnecessary calculations; and correction of one programming error. These two programs are available from the author; they have been compared with the direct matrix inverse procedure, with 11-decimal agreement in results. A simple example and sample print-outs are given in appendix B.
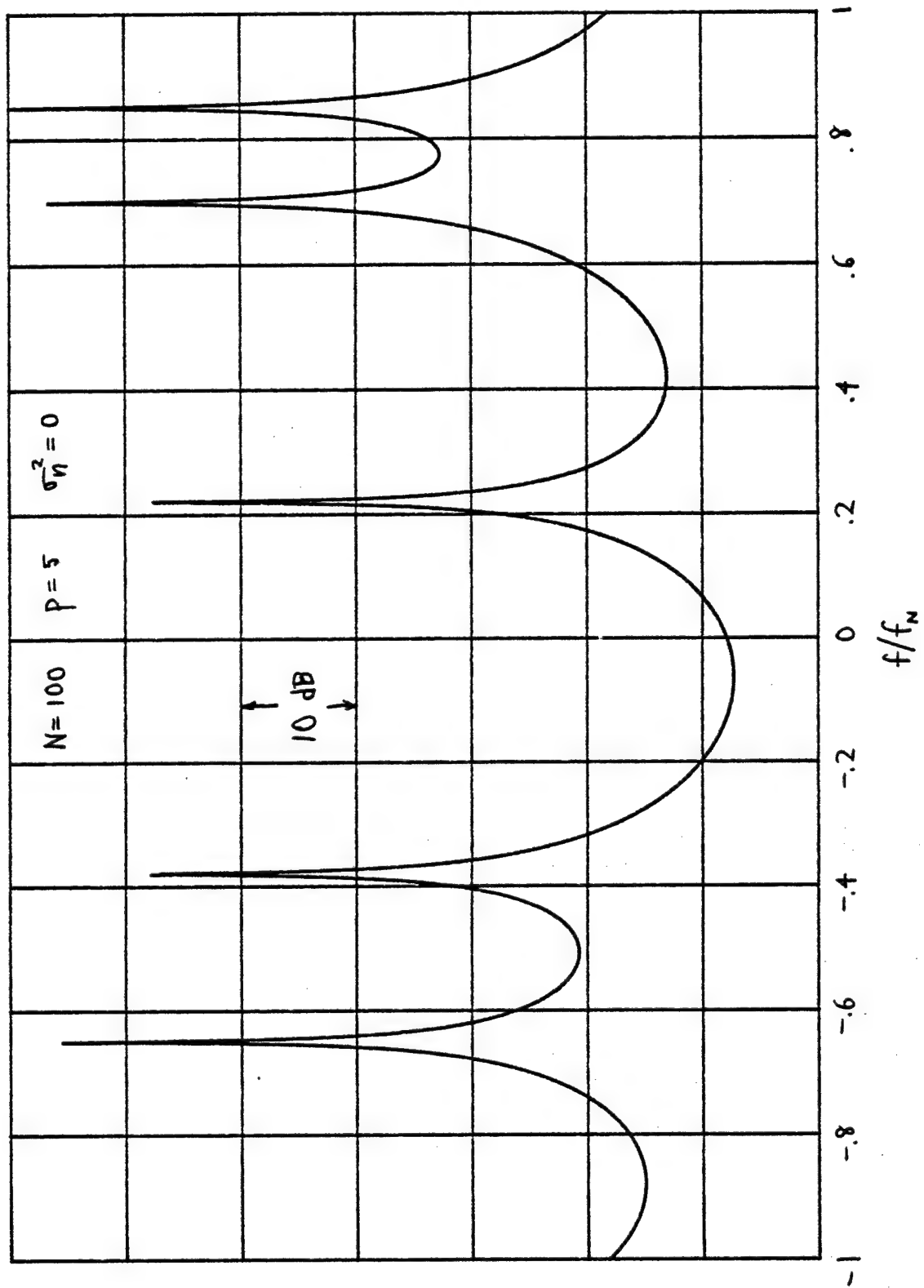
Figure 2. Five Equal-Amplitude Tones; No Noise; P=5
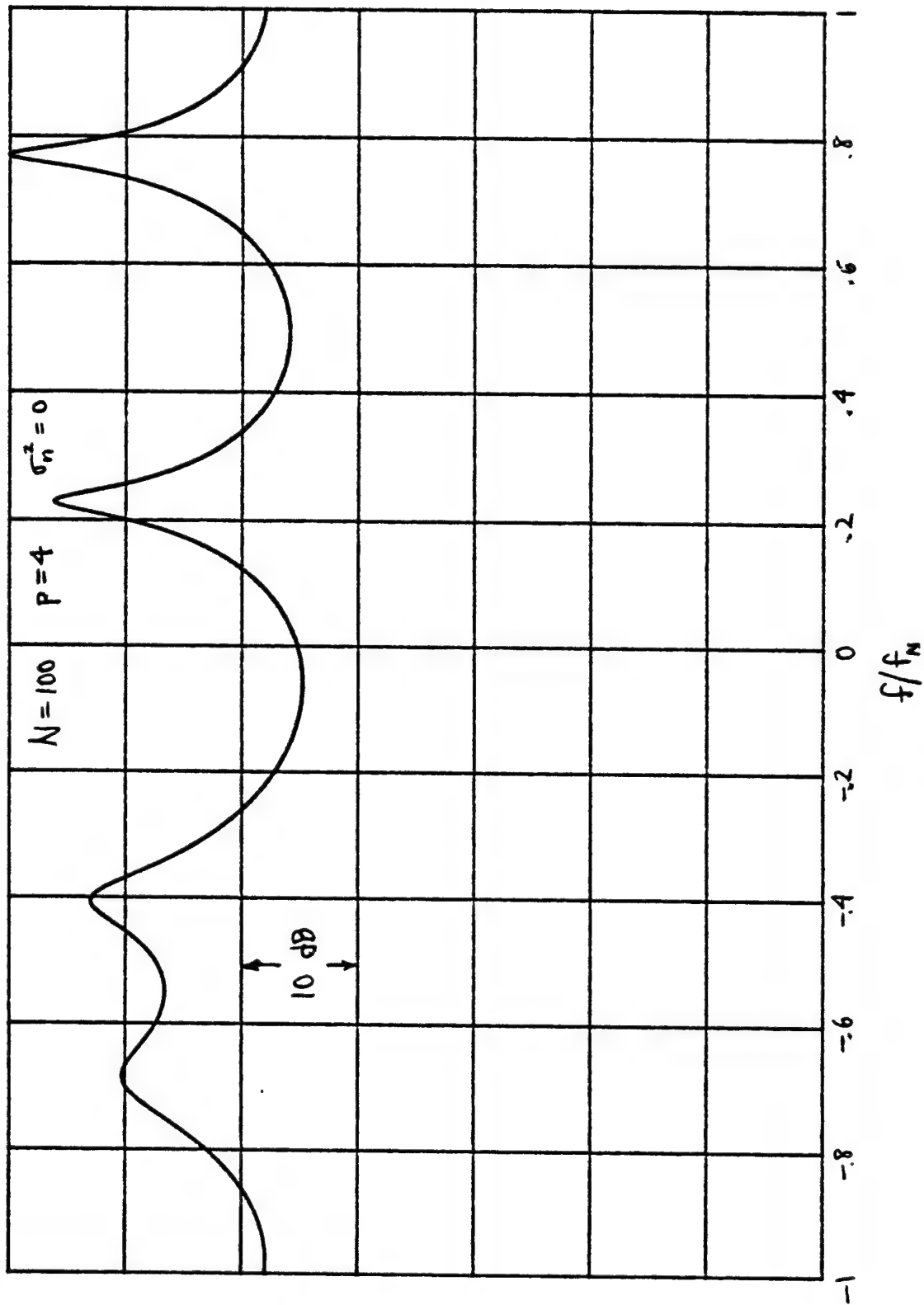
Figure 3. Five Equal-Amplitude Tones; No Noise; P=4
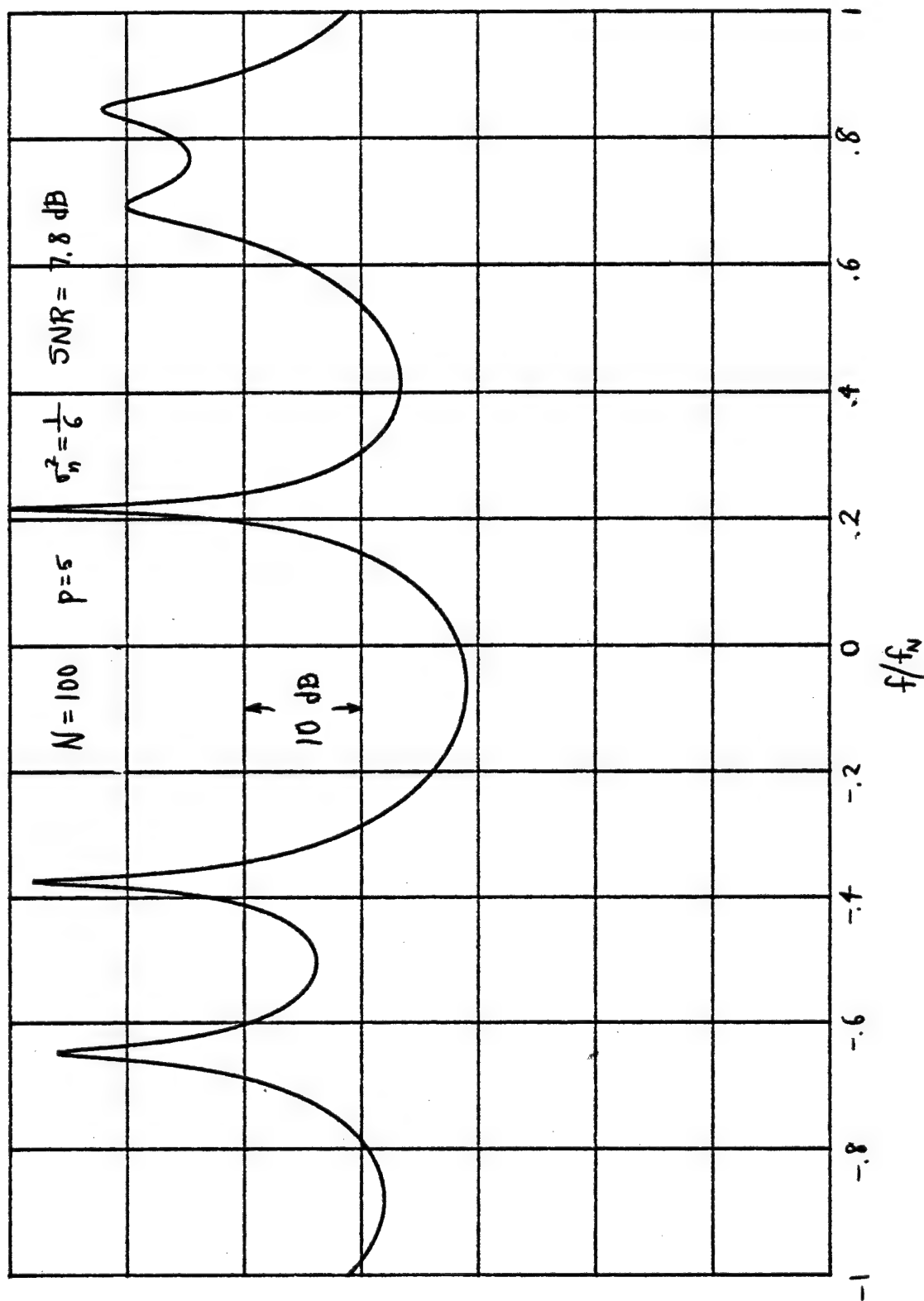
Figure 4. Five Equal-Amplitude Tones; White Noise ; P = 5

Within the figure:
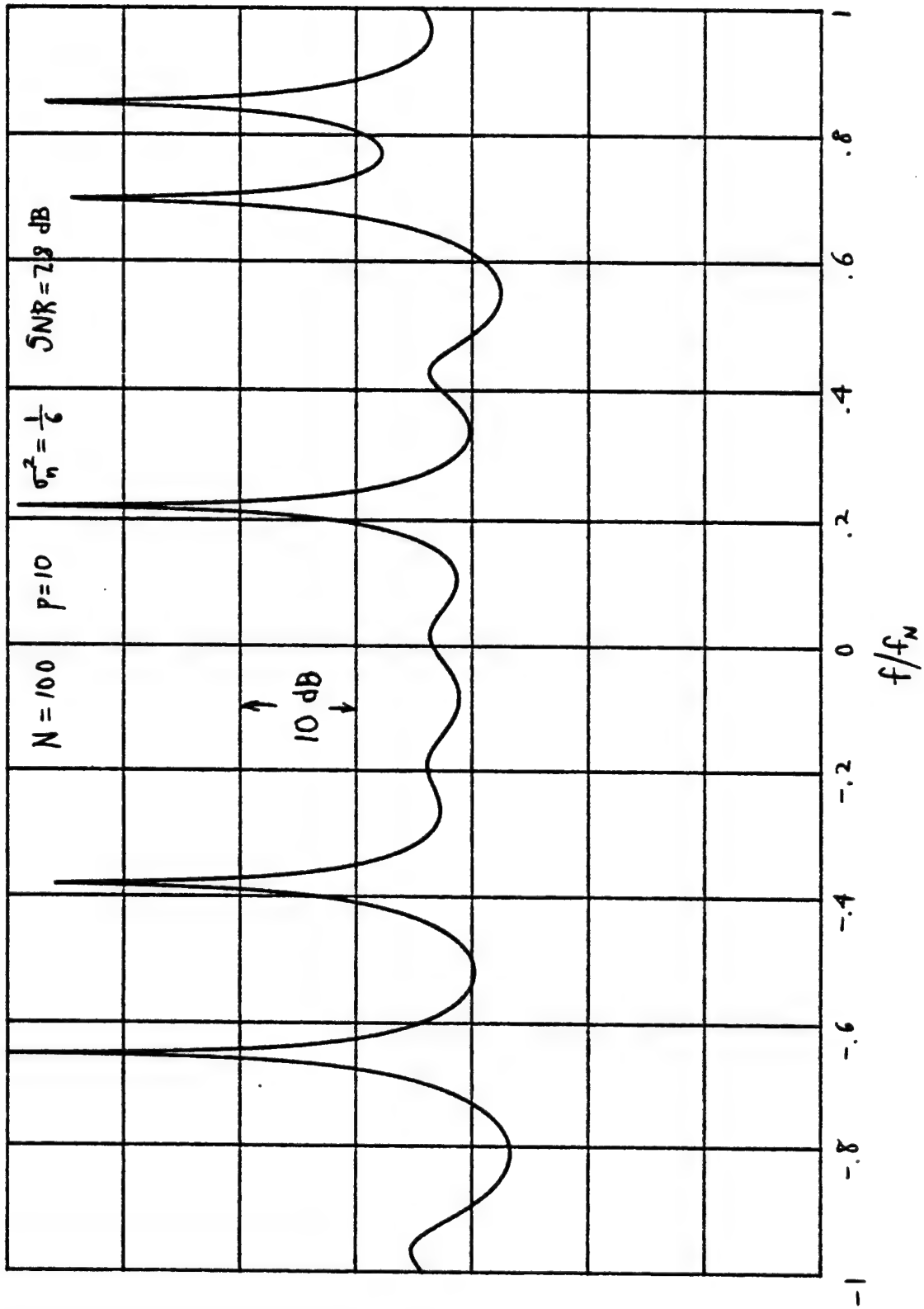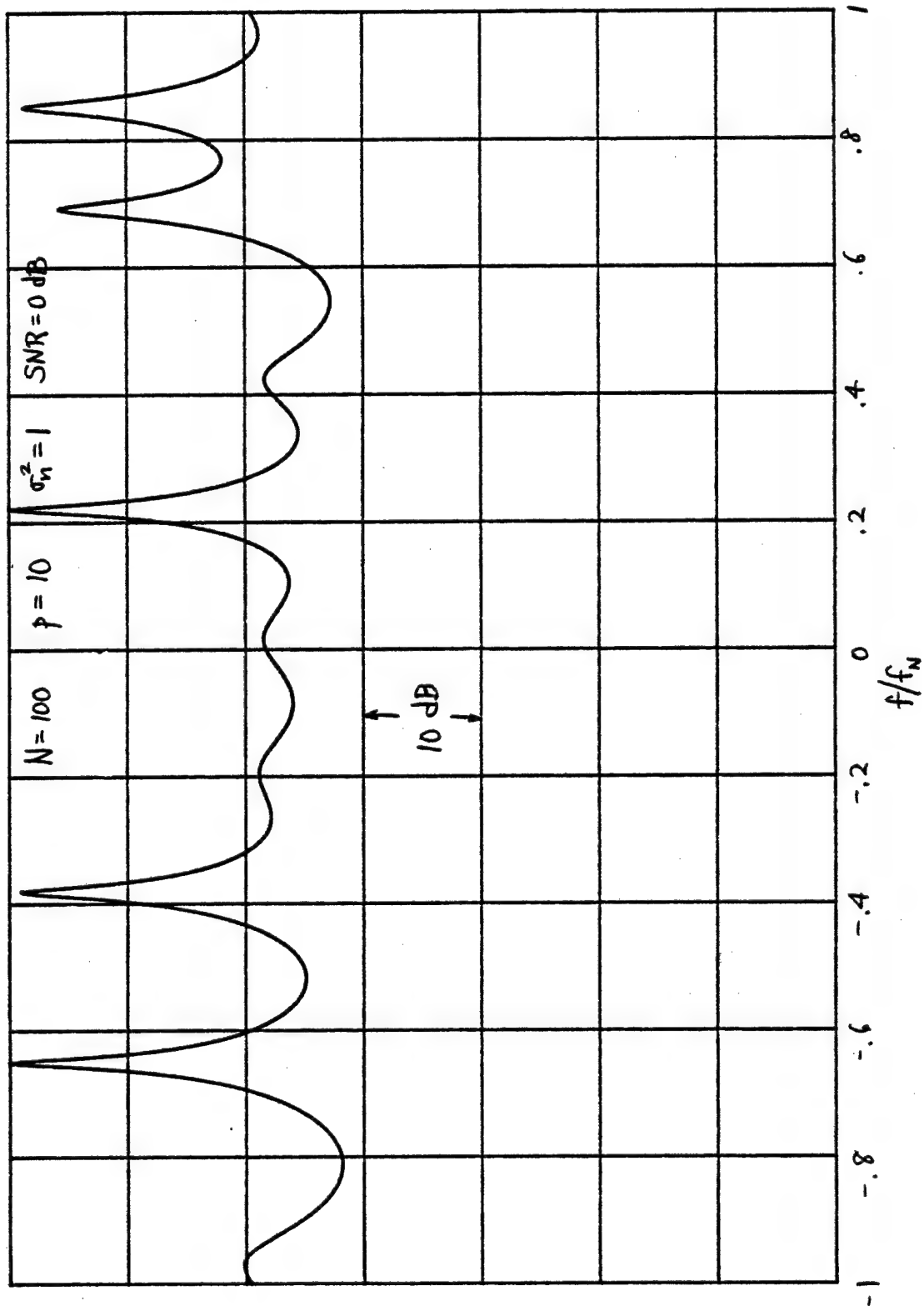$N = 100$ $P = 5$ $\sigma_n^2 = \frac{1}{6}$ $SNR = 7.8$ dB

10 dB

f/f_N

Figure 5. Five Equal-Amplitude Tones; White Noise; $p = 10$

Figure 6. Five Equal-Amplitude Tones; White Noise; $p = 10$
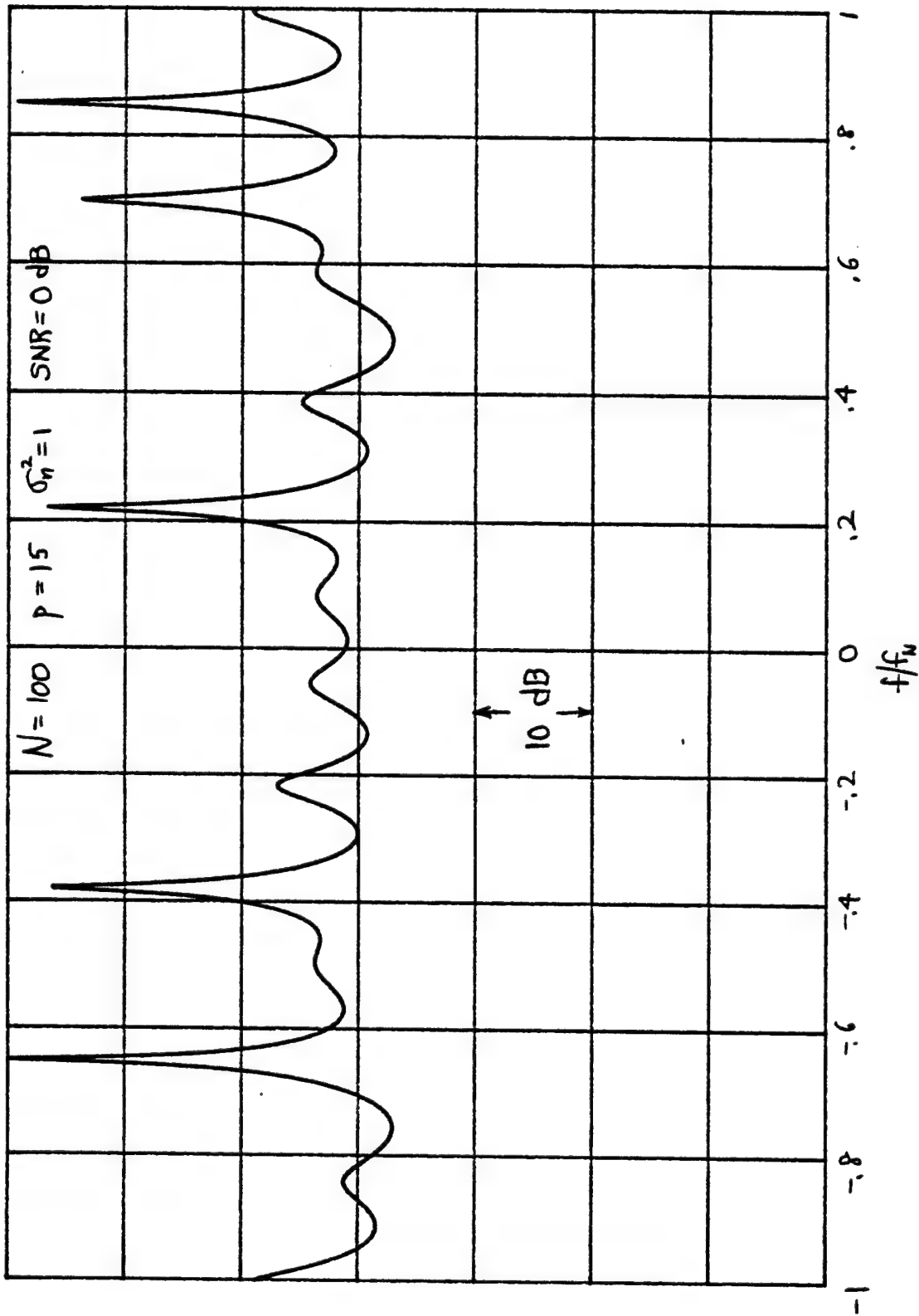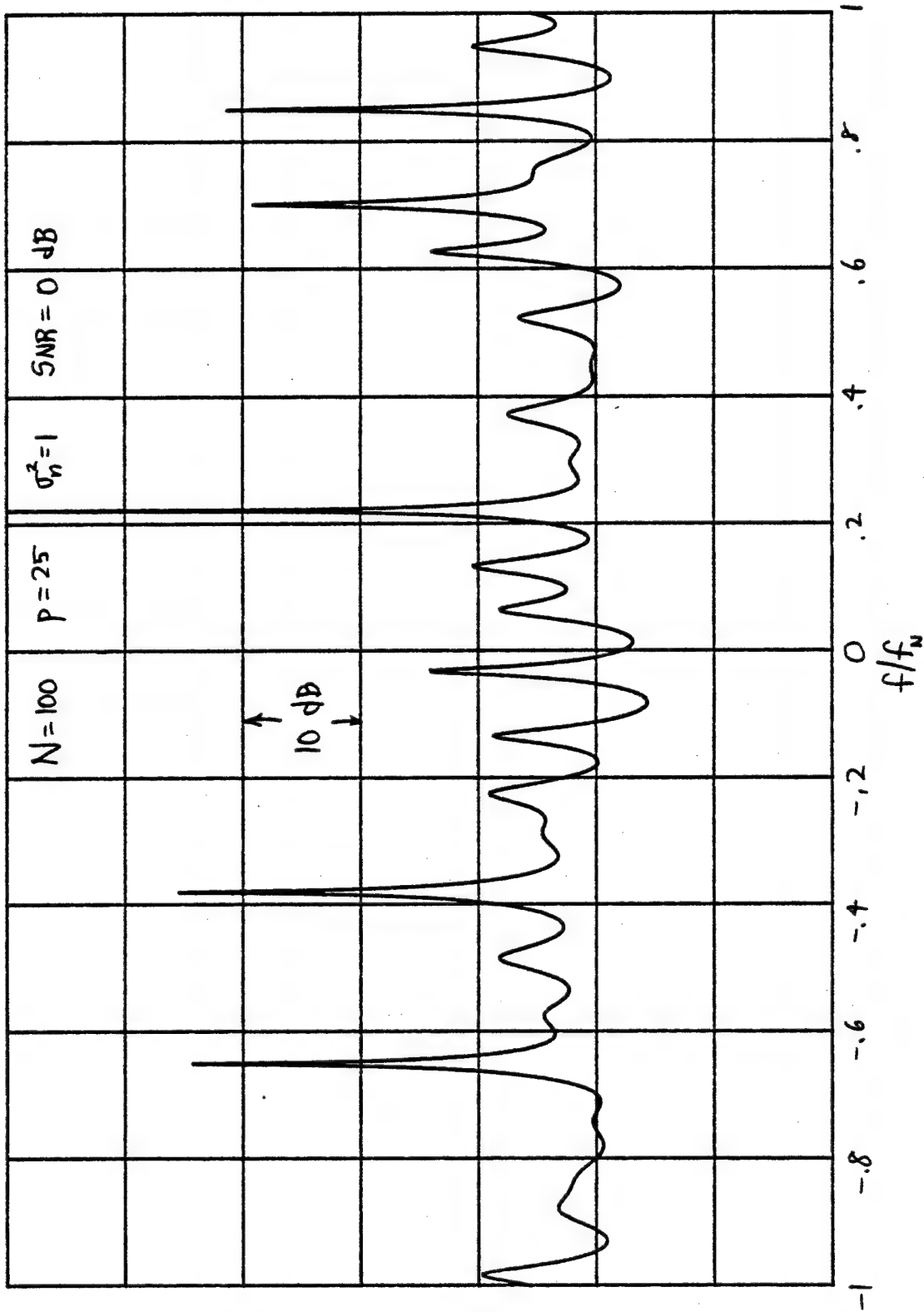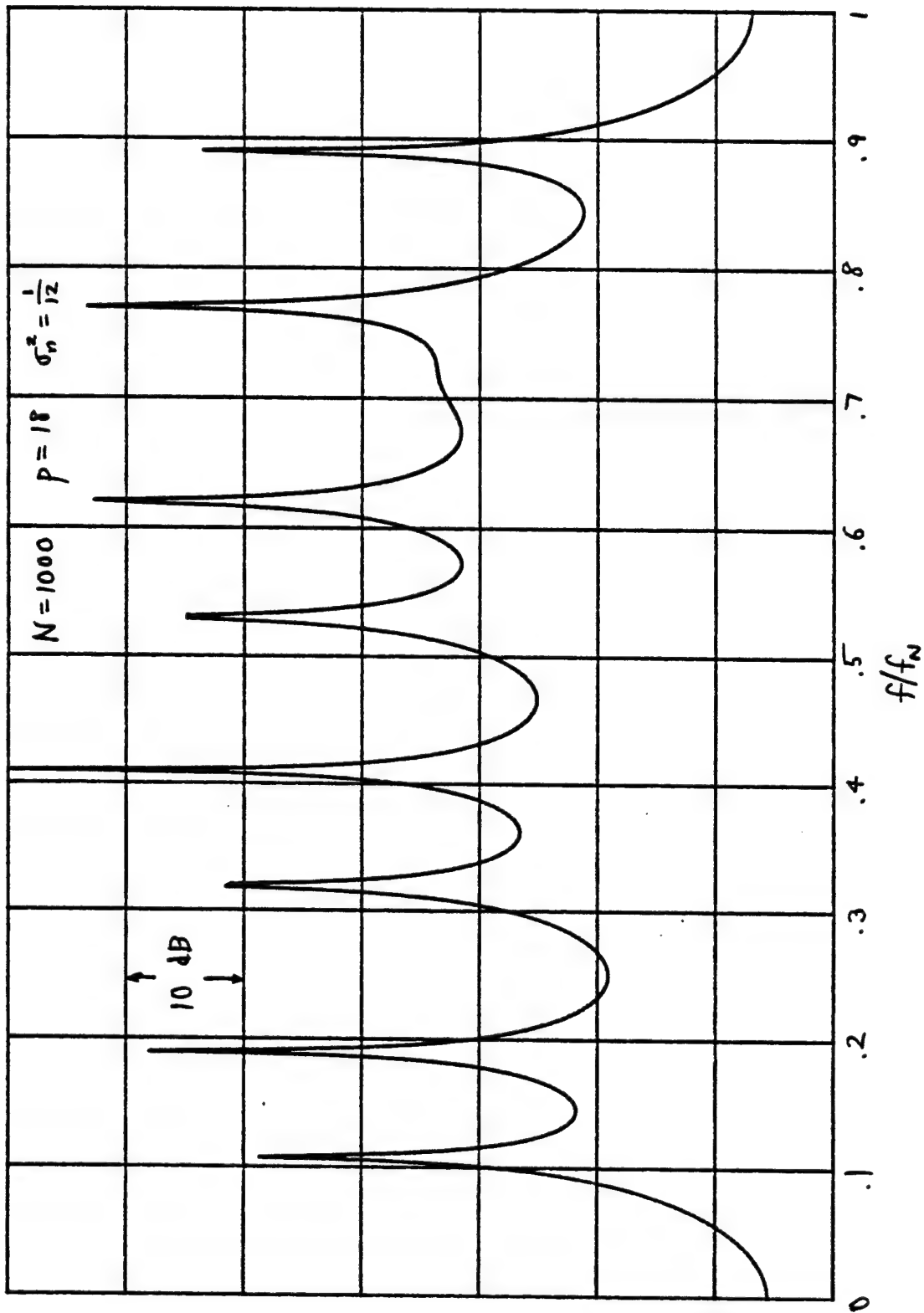
Figure 7. Five Equal-Amplitude Tones; White Noise; p = 15

Figure 8. Five Equal-Amplitude Tones; White Noise; p = 25
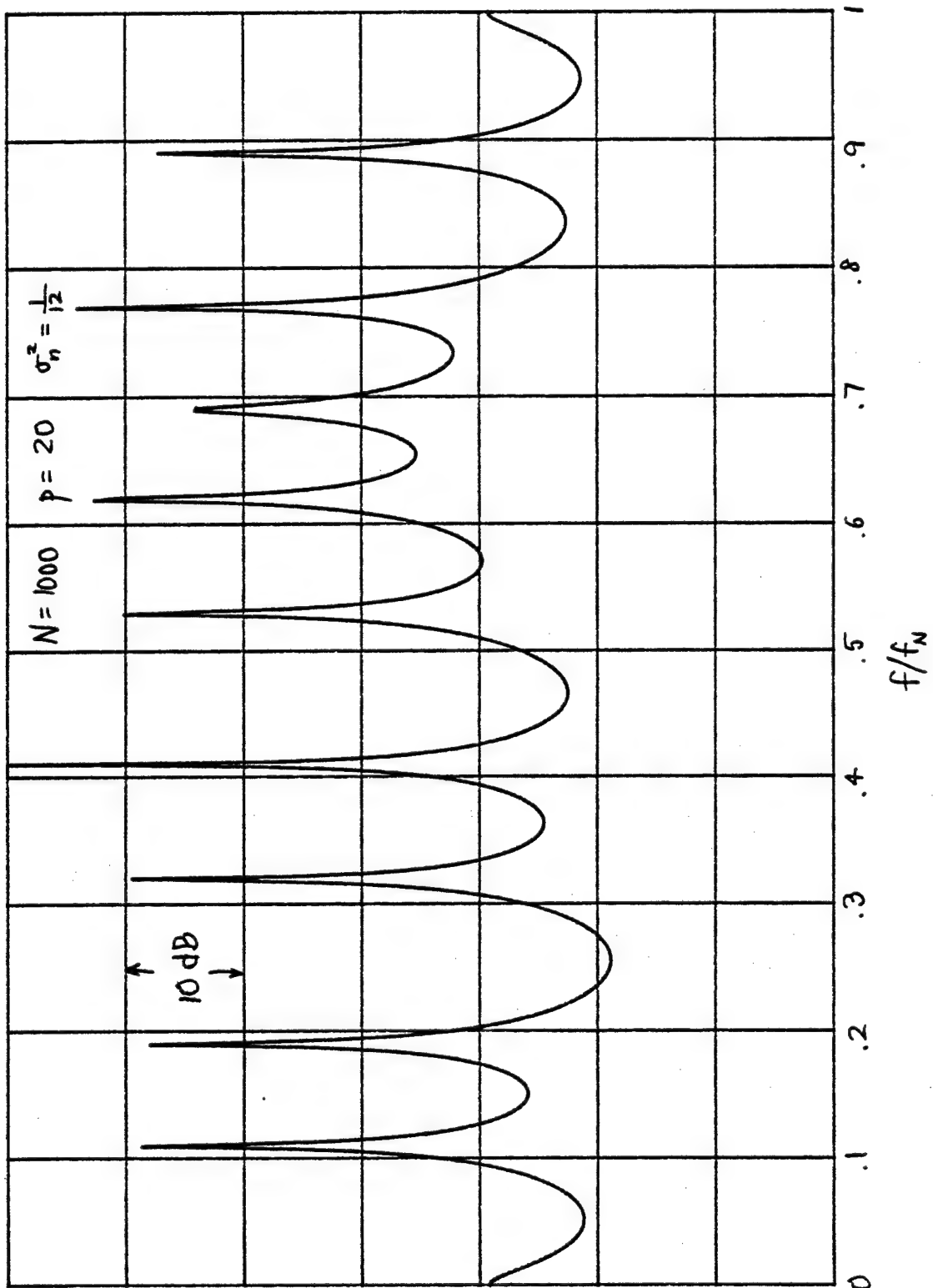
Figure 9. Nine Tones; White Noise; $p = 18$
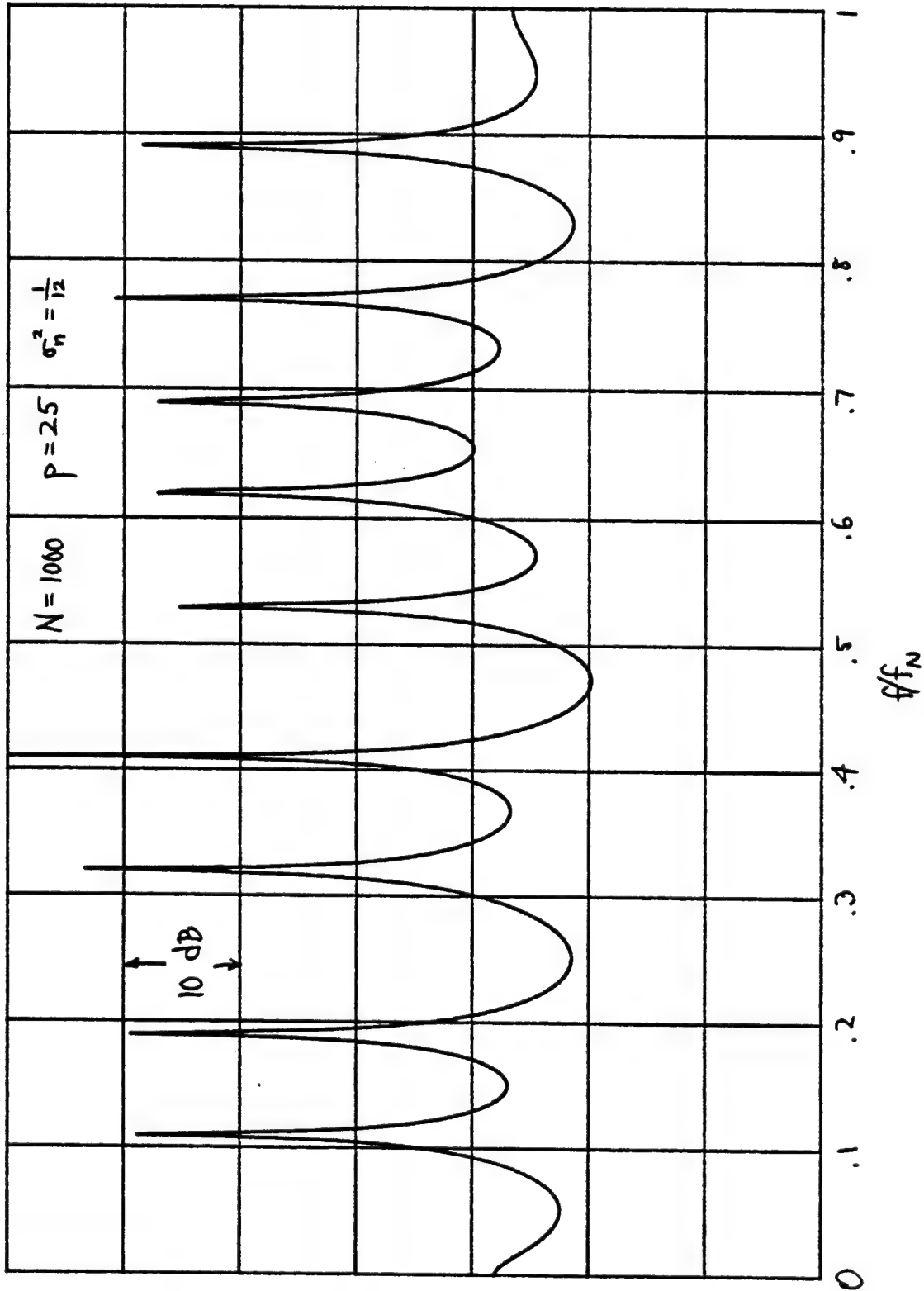
Figure 10. Nine Tones; White Noise; p = 20

$$N = 1060 \quad P = 25$$

$$\sigma_n^2 = \frac{1}{12}$$

$$10 \text{ dB}$$
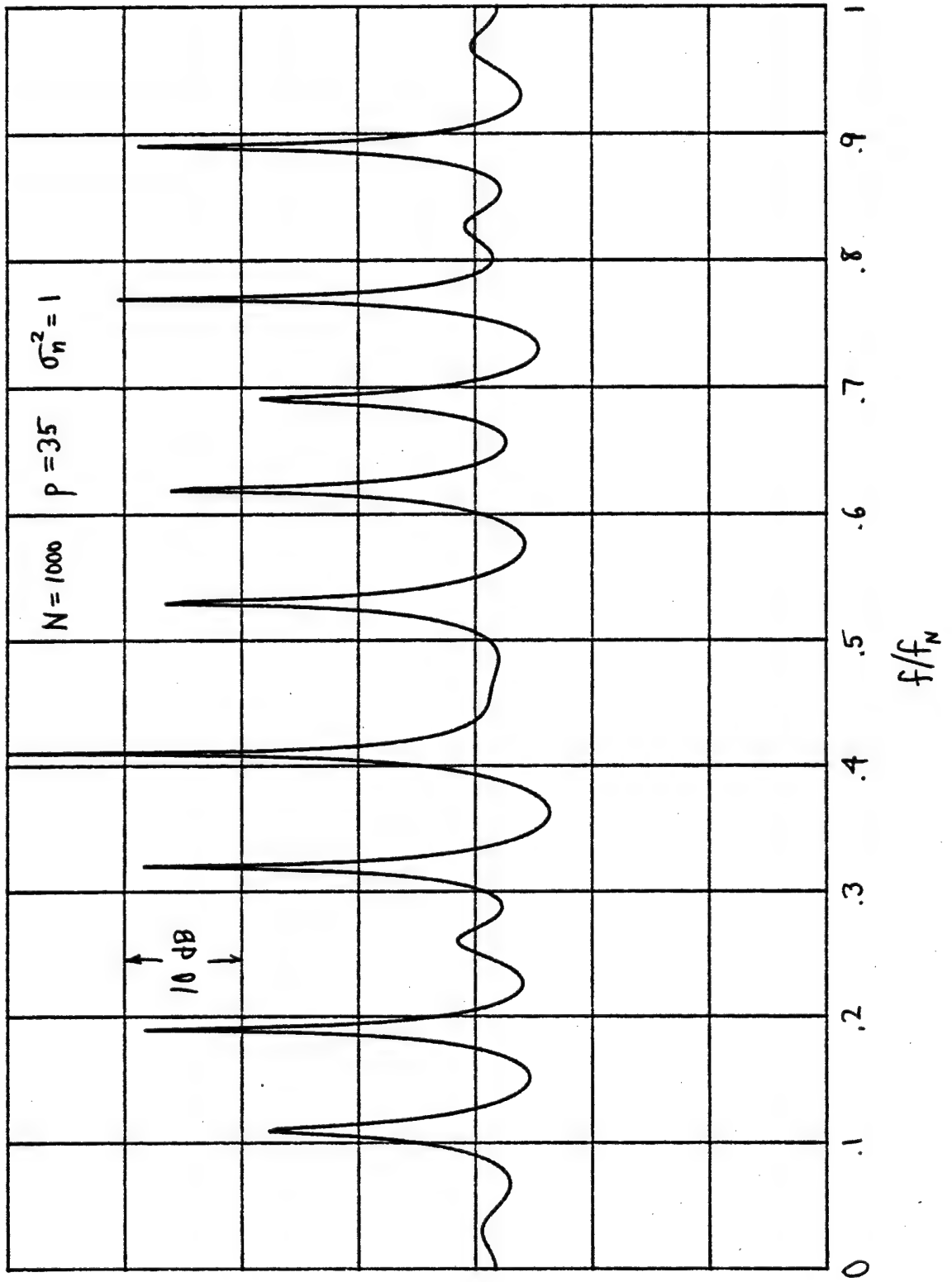
$$f/f_N$$

Figure 11. Nine Tones; White Noise; p = 25
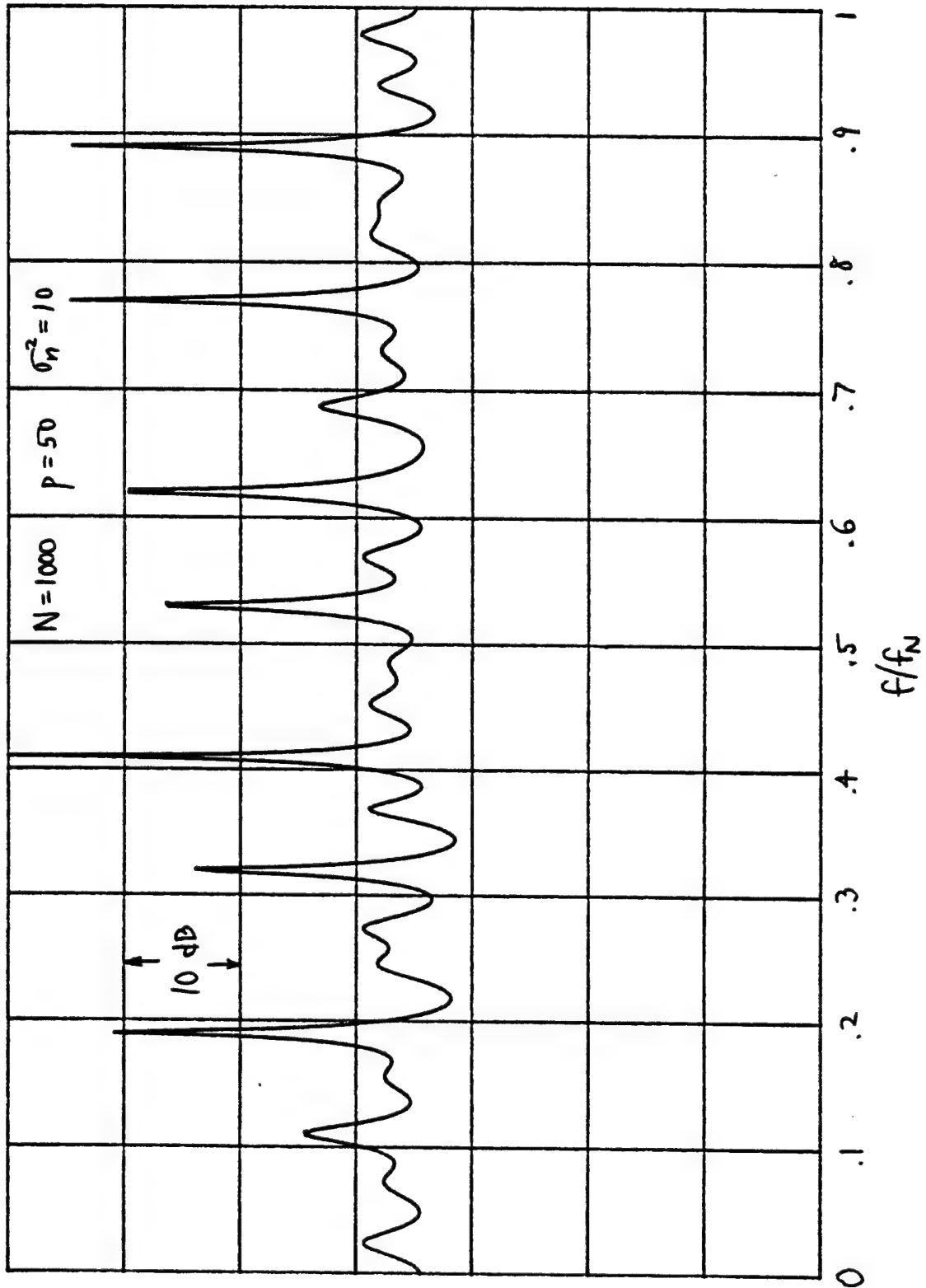
Figure 12. Nine Tones; White Noise Power = 1 ; P = 35
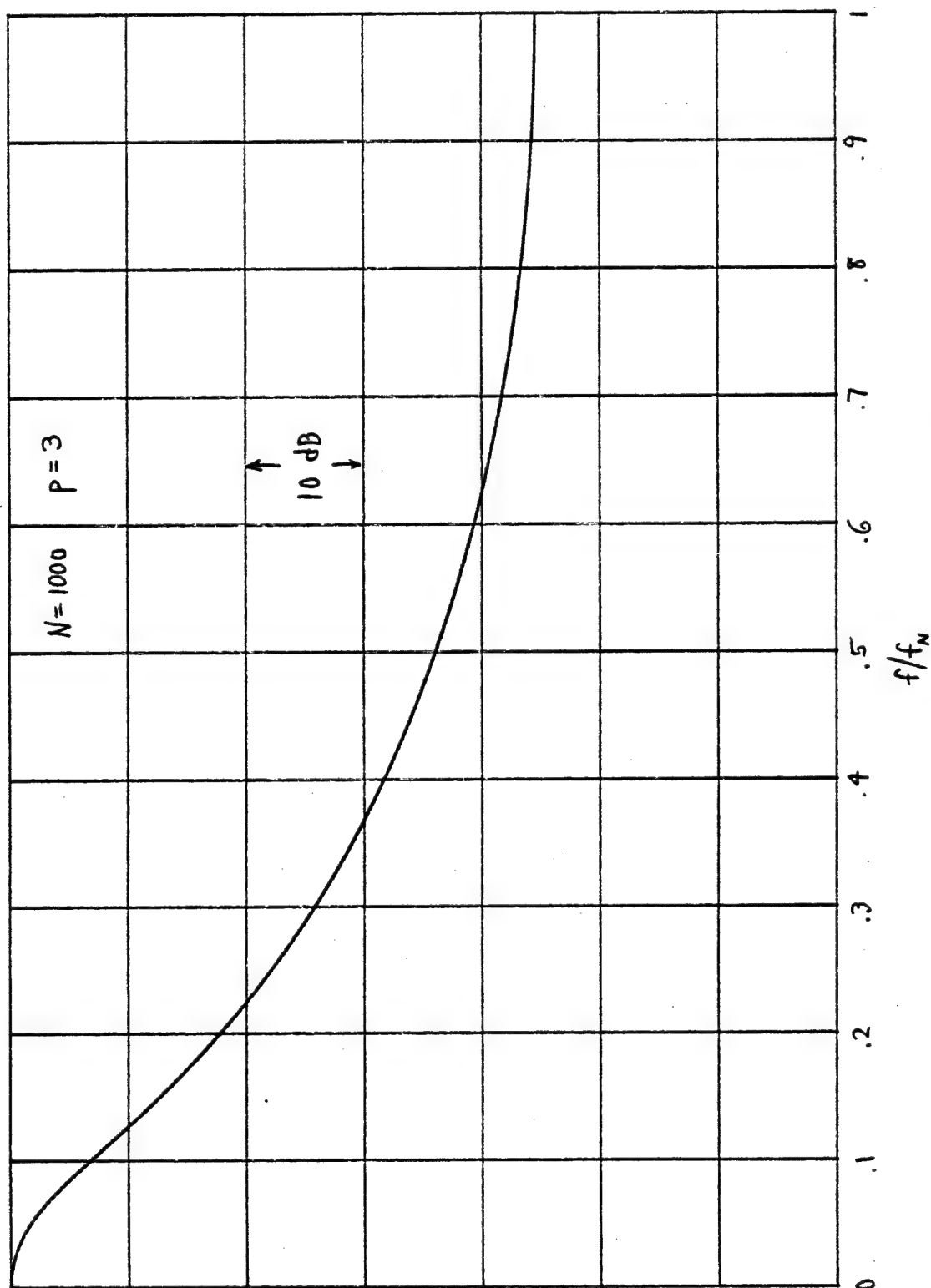
Figure 13. Nine Tones; White Noise Power = 10; $p = 50$

Figure 14. Spectrum of Colored Noise; Third-Order Autoregressive Process
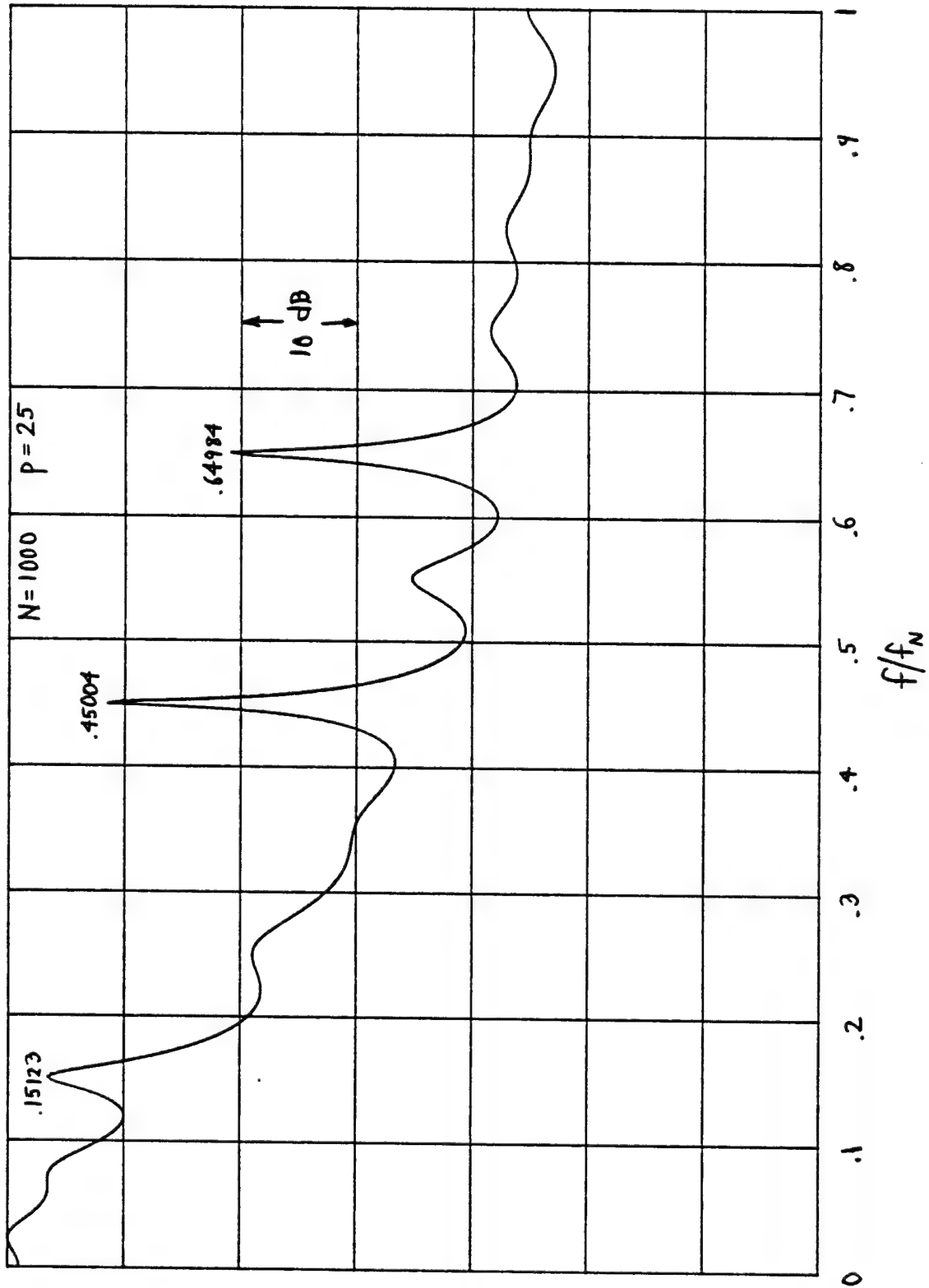
N = 1000   P = 3

10 dB

f/f_N
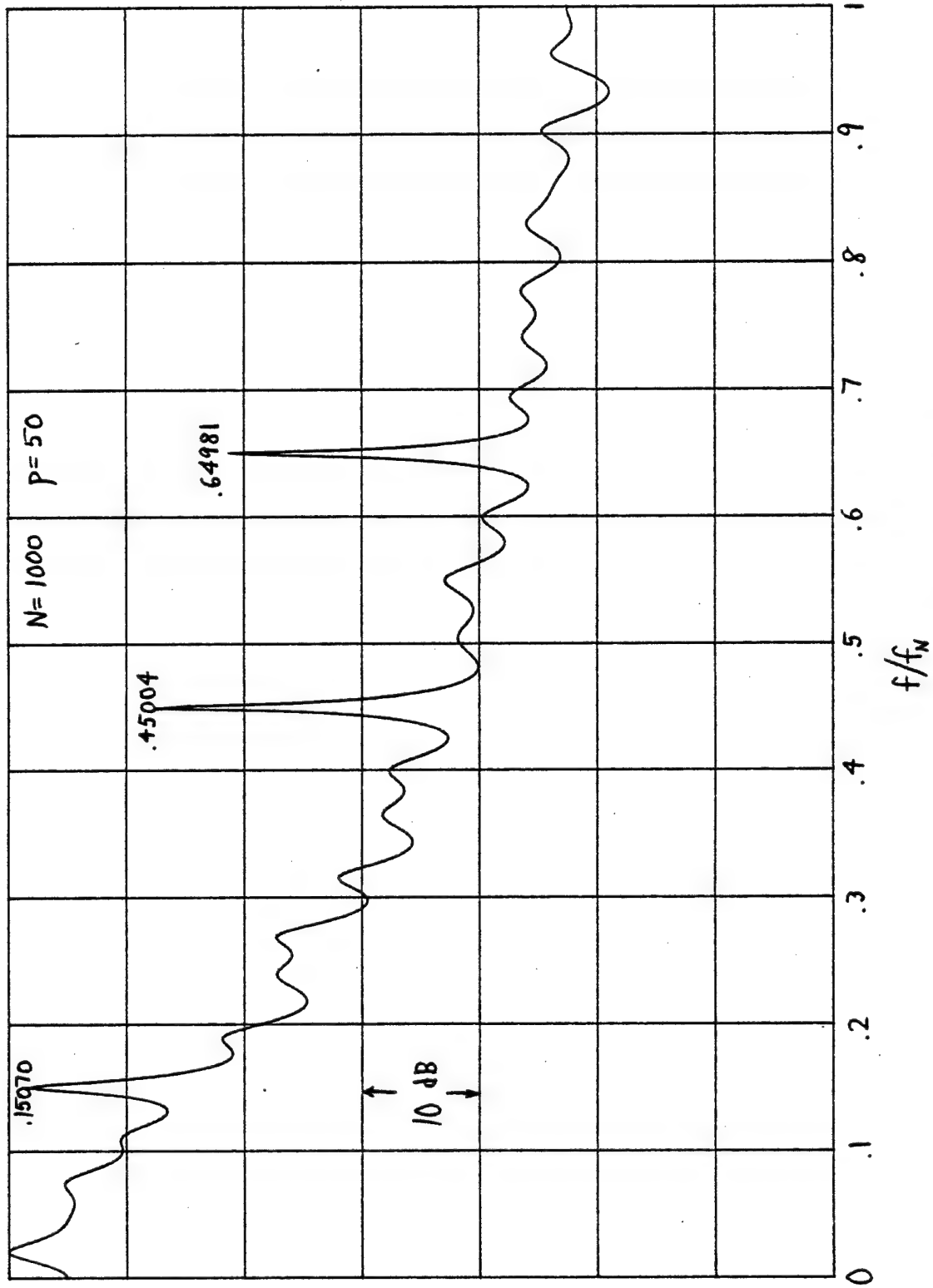
Figure 15. Three Tones with SNR = -10,-20,-30 dB; p = 25

Figure 16. Three Tones with SNR = -10, -20, -30 dB; p = 50

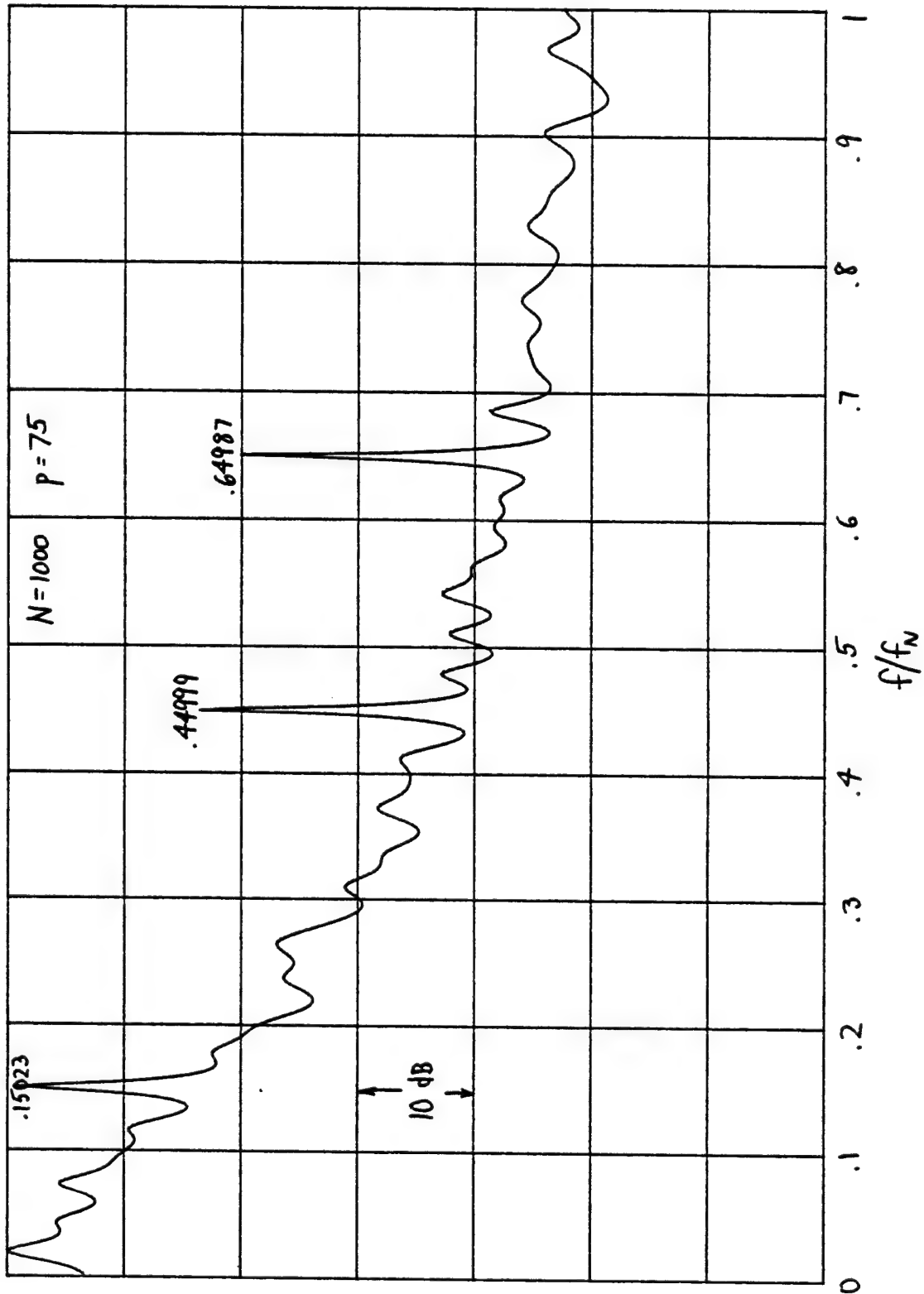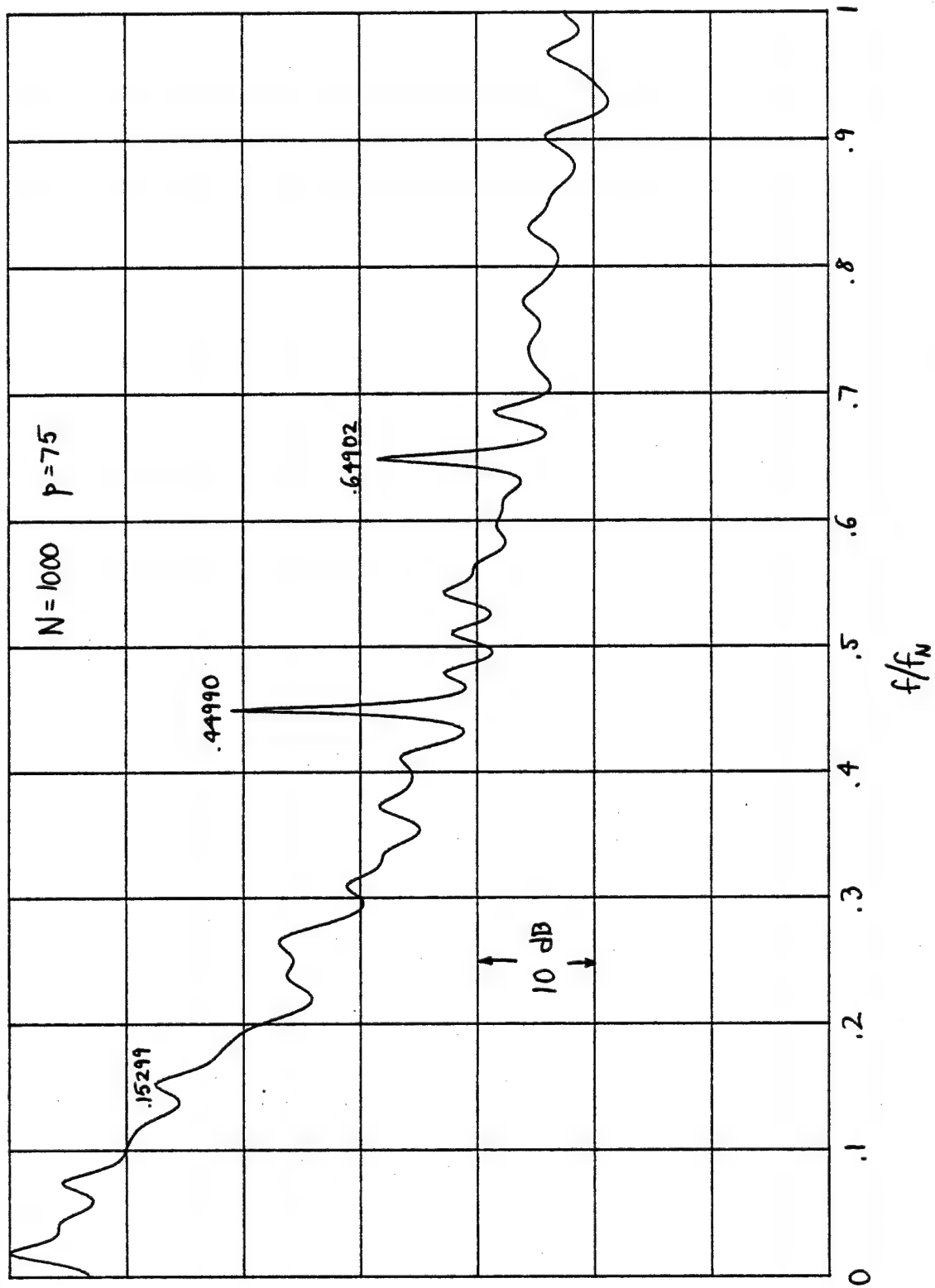Figure 17. Three Tones with SNR = -10,-20,-30 dB; p = 75

38

Figure 18. Three Tones with SNR = -20, -30, -40 dB; p = 75
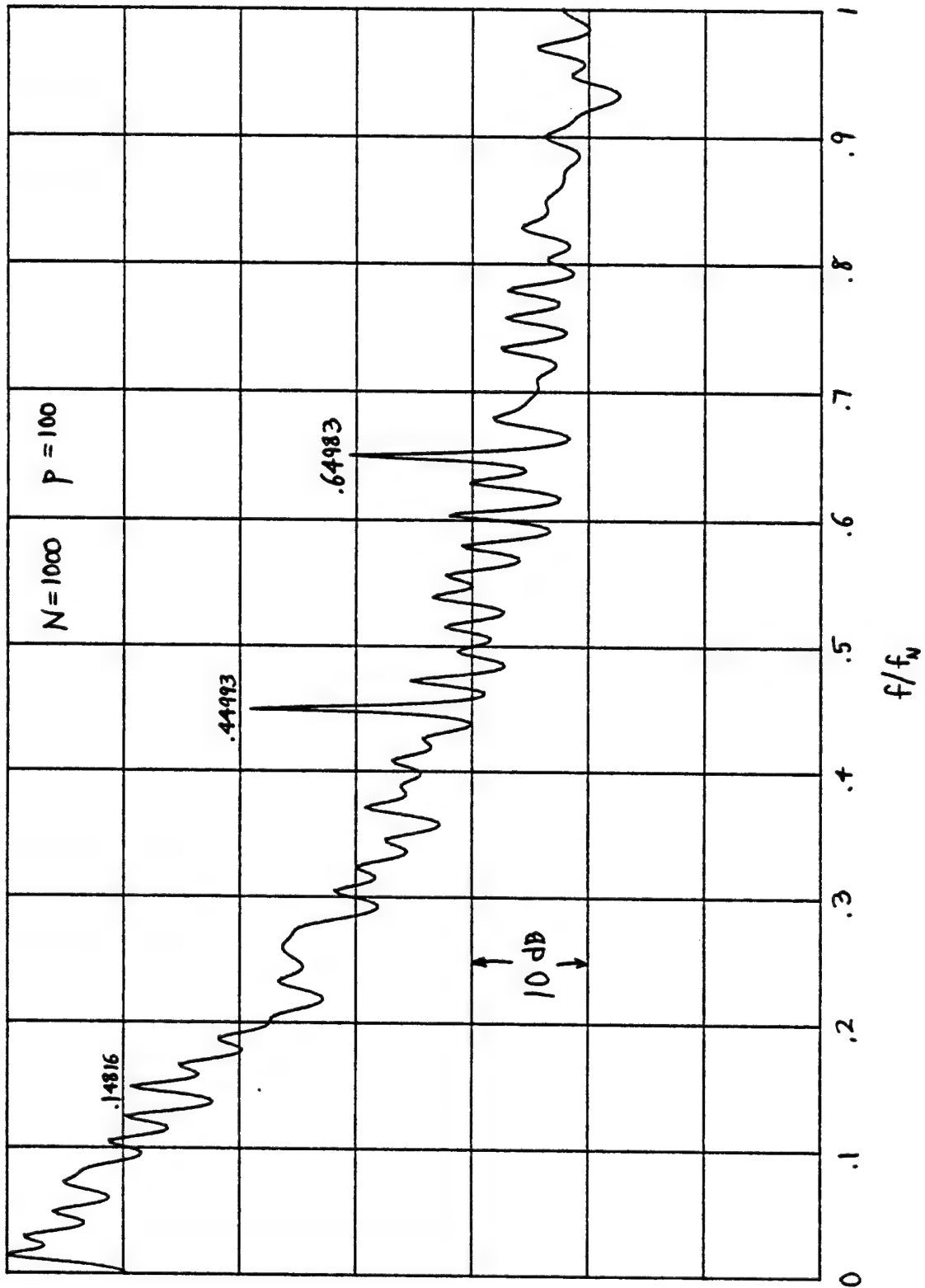
Figure 19. Three Tones with SNR = -20, -30, -40 dB; P = 100

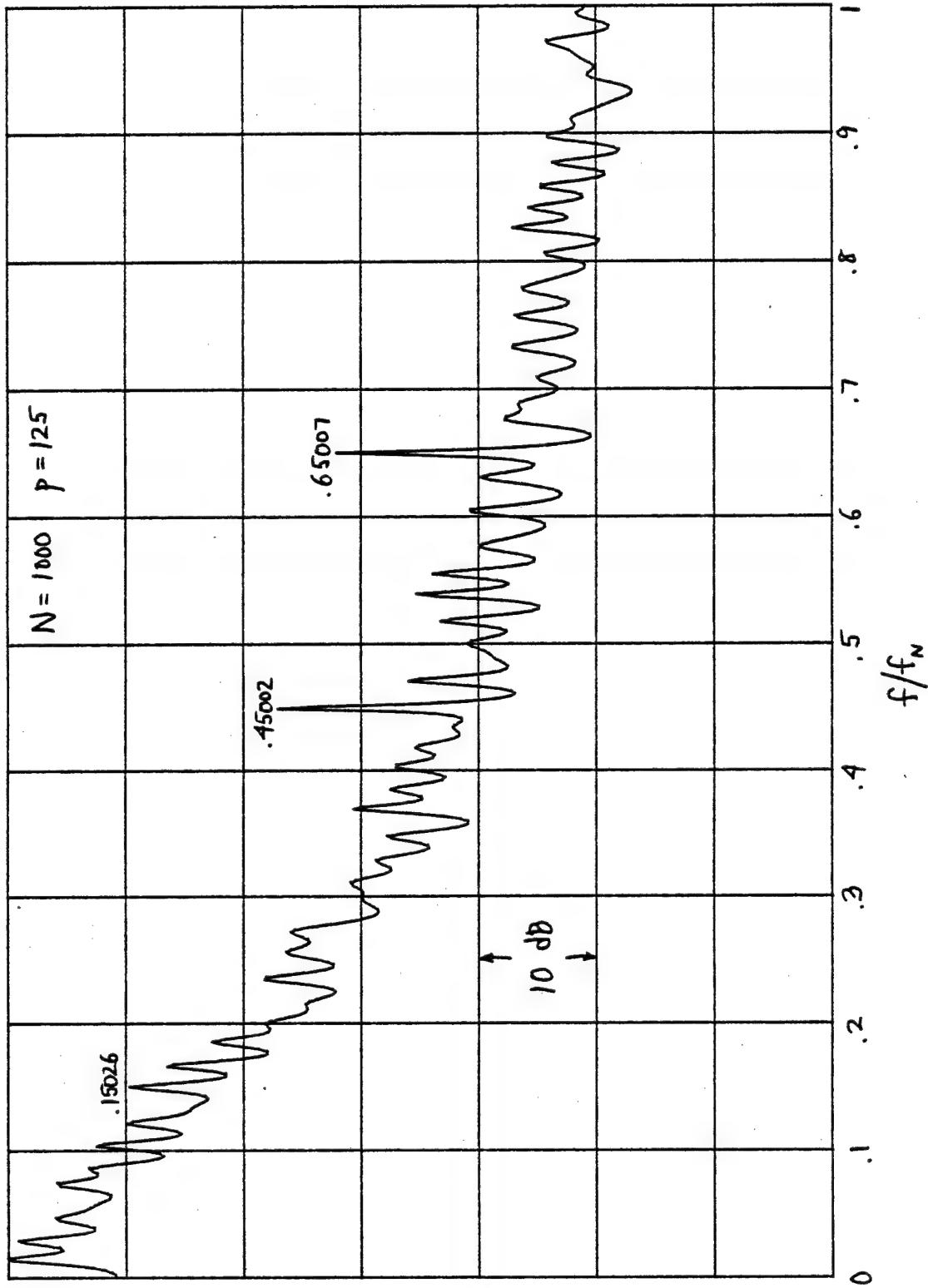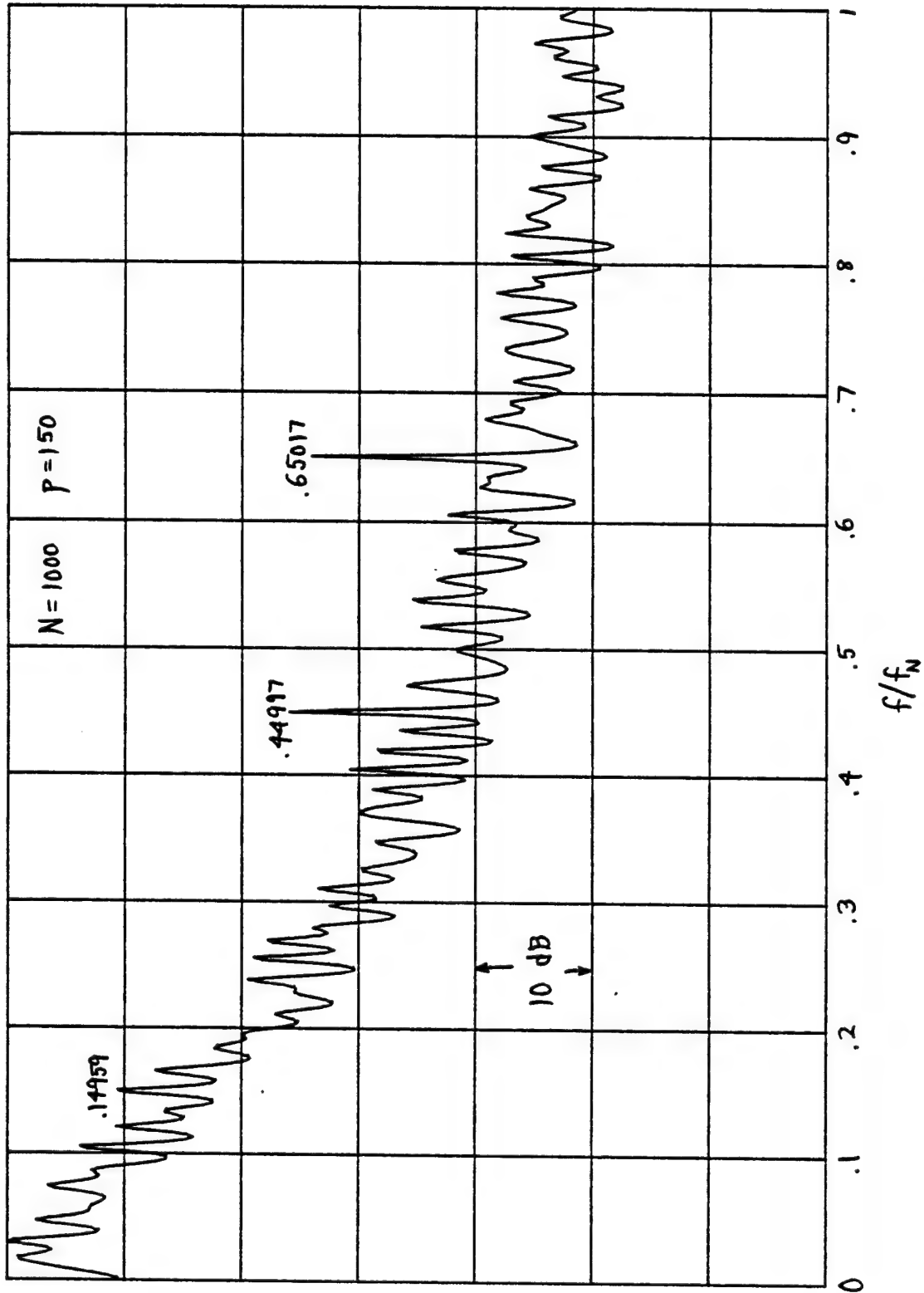Figure 20. Three Tones with SNR = -20, -30, -40 dB; p = 125

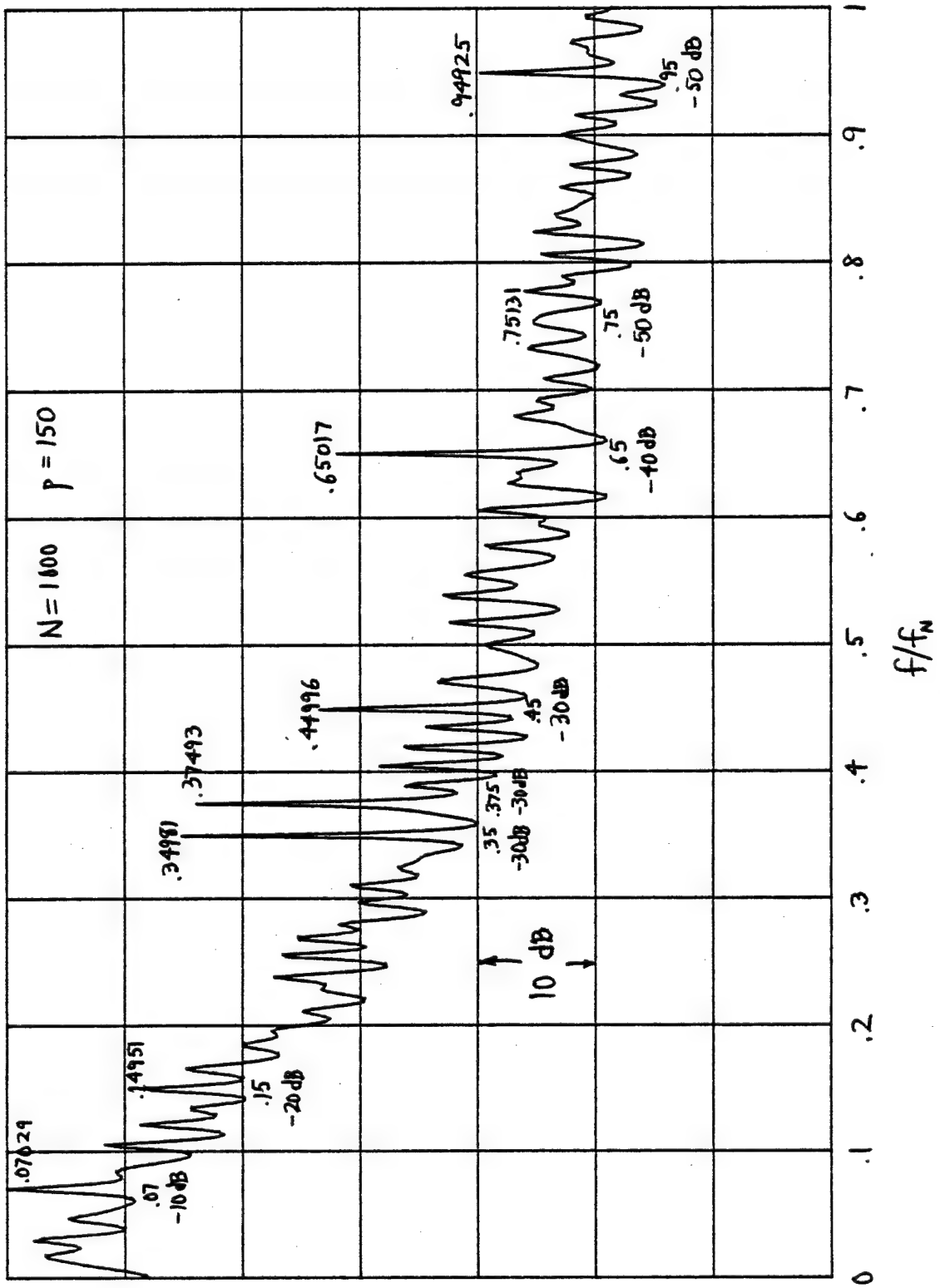Figure 21. Three Tones with SNR = -20, -30, -40 dB ; P = 150

Figure 22. Eight Tones with Various SNRs ; P = 150
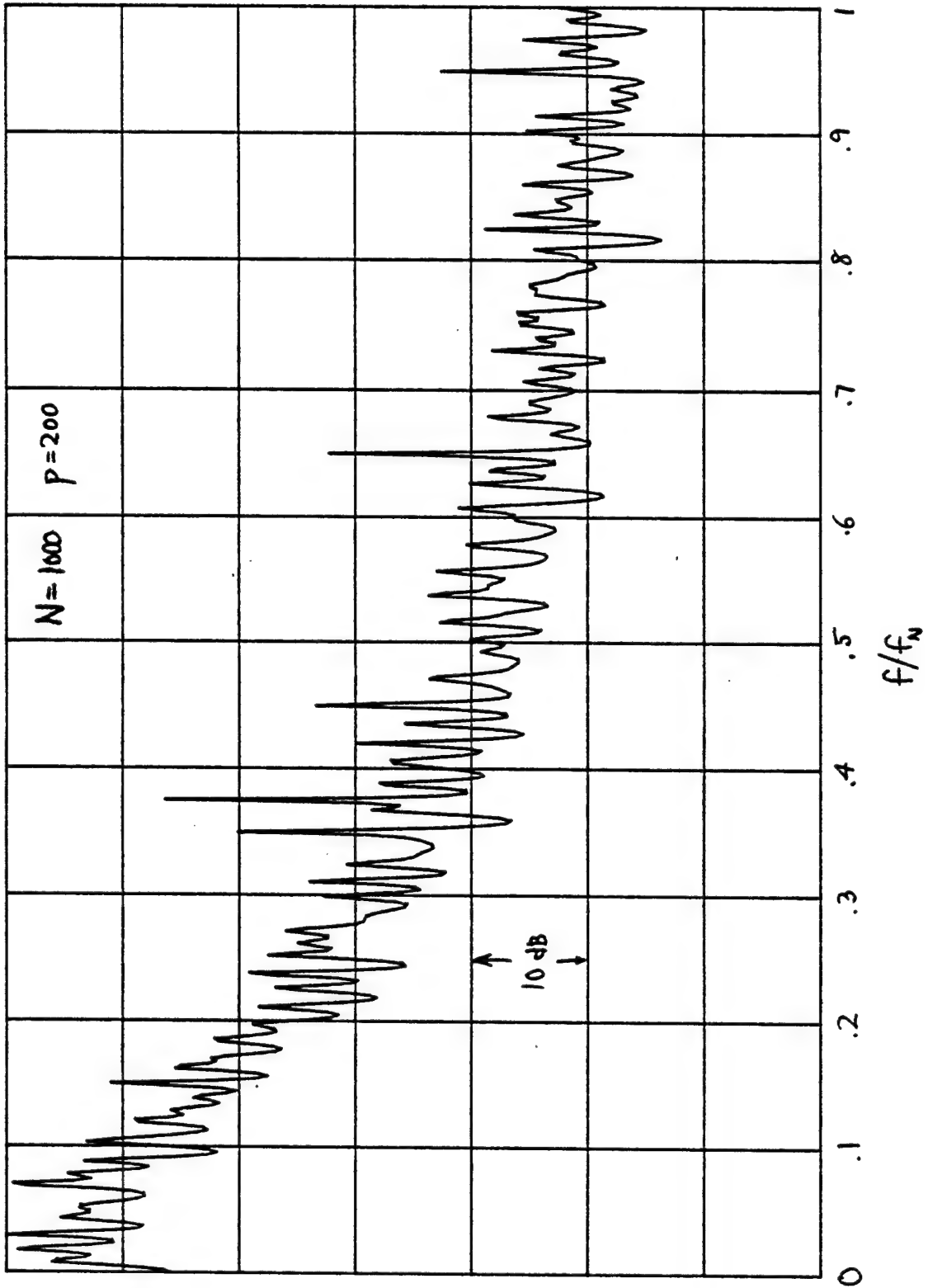
Figure 23. Eight Tones with Various SNRs; p = 200

APPENDIX A. ZERO LOCATION OF $\mathcal{A}(z)$

For a complex function $f(z)$, suppose we have evaluated $f(z)$ and its derivative at a point z_1 fairly close to a zero z_o of $f(z)$. Then we can express

$$f(z) \cong f(z_1) + f'(z_1)(z-z_1) \text{ for } z \text{ near } z_1 . \qquad (A-1)$$

We can then get an estimate of the zero location of $f(z)$ by setting (A-1) to zero; we obtain the estimate

$$z_2 = z_1 - \frac{f(z_1)}{f'(z_1)} \qquad (f'(z_1) \neq 0). \qquad (A-2)$$

This procedure can be repeated by evaluating f and f' at point z_2; the procedure converges if $f'(z_o) \neq 0$, that is, if z_o is a simple zero of $f(z)$.

For our application, $f(z)$ is given by polynomial (2). It is thus a simple matter to evaluate the function and its derivative at any point z. The starting point for this procedure is obtained as follows: we evaluate spectral estimate $P(f)$ in (1) at a large number of equally-spaced points in $|f| < \frac{1}{2\Delta}$, by means of an FFT. We then select particular frequencies where $P(f)$ is very large compared to neighboring frequency points and use these as starting points in recursion (A-2). That is, a point on the unit circle in figure 1 very close to ζ_o is used as starting point z_1. Recursion leads to the closest zero of $\mathcal{A}(z)$, namely z_o.

APPENDIX B. FIVE-TONE EXAMPLE, PRINT OUT, AND INTERPRETATION

The example of interest here is the one given in (23), namely five equal-amplitude complex exponentials

$$X_n = \sum_{k=1}^{5} \exp\left(i 2\pi f_k \Delta n\right) , \quad 1 \leq n \leq N = 100, \qquad \text{(B-1)}$$

where

$$\frac{f_k}{f_N} = 2\Delta f_k = -.65, -.38, .22, .70, .85 . \qquad \text{(B-2)}$$

The first method of processing the data is: subtract the sample mean and then employ the F&B procedure. The computer print-out results are presented in table B-1, and are interpreted as follows. The sample mean of the data is complex and is given by the number $-.02 - i.003727$. The sample variance of the data is 4.8796. The least-squares algorithm has several different ways of terminating its recursive procedure; the criterion encountered here is status 1, which indicates that the maximum specified order of 5 was realized without satisfying any of the stopping criteria. The prediction-error power of the best prediction-filter is .00837. The best filter weights are complex and given by the five pairs of numbers listed together. The variance from the graph is realized by numerically integrating under the spectral estimate (1) by means of the Trapezoidal rule, at the FFT points computed, and using the prediction-error power given above. The locations of the poles are specified by their real, imaginary, magnitude, and argument/π values, respectively. The power content of each pole and its 3dB bandwidth are evaluated according to (11) and (6). And the amplitude of the corresponding tone is accomplished according to

(14). These are the results quoted in table 1 in the main body of this memorandum.
The corresponding spectral plot in figure 2 is reproduced here in figure B-1 for
easy reference and comparison to the following results.

It was noted that subtraction of the sample mean from a set of data can
create an effective dc component in the original process, and thereby require an
additional order in the filter for its prediction. This is the reason that the
prediction-error power of .00837 above is not zero. When we increase the filter
order to 6, the results of table B-2 and figure B-2 are obtained. We notice a
significant dc indication in the figure and a nearly-zero prediction error power
of -2.1E-10; round off error has led to this very small negative number, corresponding
status indicator 4, and a negative variance from the graph. We also notice that for
this noise-free case, all six poles are now on the unit circle and have exactly
the correct frequency, except for round-off error. The last pole is actually just
outside the unit circle near z=1, and corresponds to the created dc component noted
earlier. The power content and bandwidth outputs are spurious for this example,
due to round-off error.

Lastly, we consider the effect of not subtracting off the sample mean, but
keeping p at 5, the results of which are given in table B-3 and figure B-3. We
again see perfect pole location estimation , as predicted by (16)-(18), and a
negative prediction-error power of -3.45E-11, due to round-off error. The spectral
plots in figures B-1 through B-3 are very similar, except for the dc indication in

figure B-2, for reasons indicated above.

When noise is added to the tones, the significance of removing or leaving the sample mean in the data becomes far less. It appears that the only time it is important, is when the true dc component is very large, in which case the sample mean should be removed so as not to contaminate the spectral estimate in the neighborhood of zero frequency. All the results in the main body of this memorandum have had the sample mean removed.

LINEAR PREDICTIVE SPECTRAL ANALYSIS FOR COMPLEX DATA.
FORWARD AND BACKWARD AVERAGING. MARPLE ALGORITHM, 5 DEC 79.
FILTER WEIGHTS; SPECTRUM; POLE LOCATIONS AND POWERS.
NUMBER OF COMPLEX DATA POINTS = 100
MAXIMUM ORDER OF FILTER = 5

MEAN OF DATA = -2.00000000267E-02 -3.72722031951E-03
VARIANCE OF DATA = 4.87958610779

STATUS OF STOPPING CRITERION = 1
PREDICTION-ERROR POWER = 8.37016559879E-03
OPTIMUM ORDER OF FILTER = 5
PREDICTION-FILTER WEIGHTS:
-.792285088326   .078899668937
-.73638337304   -.262804443791
-.312567503922   .717233865238
-.601825004587   .522847752701
-.683323945939   .726785507267

VARIANCE FROM GRAPH = 1.76044711955

LOCATIONS OF POLES: REAL,IMAG,MAG,ARG/PI

-.453612913509   -.890878000423   .999714102602   -.64991145804
Power content of pole = .970737957165   3 dB Bandwidth = 1.82007937708E-04
Amplitude of tone = .970052170292

.368261571624   -.929531300933   .999822496522   -.379930705775
Power content of pole = .967105663768   3 dB Bandwidth = 1.13002225032E-04
Amplitude of tone = .98026470855

.7703439768   .637496046889   .999915522625   .220052021064
Power content of pole = .944648910787   3 dB Bandwidth = 5.37799640595E-05
Amplitude of tone = .979975939701

-.58706968772   .808430154109   .999104665342   .69992545898
Power content of pole = .999496115623   3 dB Bandwidth = 5.69987747441E-04
Amplitude of tone = .981047207863

-.890208035527   .453382769306   .999012653582   .85005702917
Power content of pole = .994133376834   3 dB Bandwidth = 6.28564253147E-04
Amplitude of tone = .970736291359

Table B-1. Sample Mean Subtracted; p = 5

Figure B-1. Sample Mean Subtracted; $\gamma = 5$

LINEAR PREDICTIVE SPECTRAL ANALYSIS FOR COMPLEX DATA.
FORWARD AND BACKWARD AVERAGING. MARPLE ALGORITHM, 5 DEC 79.
FILTER WEIGHTS; SPECTRUM; POLE LOCATIONS AND POWERS.
NUMBER OF COMPLEX DATA POINTS = 100
MAXIMUM ORDER OF FILTER = 6

MEAN OF DATA = -2.00000000267E-02 -3.72722031951E-03
VARIANCE OF DATA = 4.87958610779

STATUS OF STOPPING CRITERION = 4
PREDICTION-ERROR POWER =-2.13350977671E-10
OPTIMUM ORDER OF FILTER = 6
PREDICTION-FILTER WEIGHTS:
  .205855531979   .079648465162
  .056681548087   -.343054271582
  .424649388142   .981306806687
 -.288876981211   -.193517751776
 -.082856558201   .204585335696
  .684547108345   -.728968642649

VARIANCE FROM GRAPH =-43.4339553489

LOCATIONS OF POLES: REAL,IMAG,MAG,ARG/PI

-.453990499742   -.891006524193   1   -.65
Power content of pole = 0   3 dB Bandwidth = 0
Amplitude of tone = .969947470875

 .363124552692   -.929776485888   1   -.379999999997
Power content of pole = 0   3 dB Bandwidth = 0
Amplitude of tone = .980342883582

 .770513242771   .637423989744   .999999999995   .219999999999
Power content of pole = 0   3 dB Bandwidth = 0
Amplitude of tone = .980010321796

-.587785252284   .809016994384   1   .69999999999
Power content of pole = 0   3 dB Bandwidth = 0
Amplitude of tone = .981164116999

-.891006524185   .453990499756   1   .84999999999
Power content of pole = 0   3 dB Bandwidth = 0
Amplitude of tone = .970830660887

 1.00000001274   -8.64367941244E-09   1.00000001269   -2.75136857492E-09
Power content of pole = 4.08994794443E-04   3 dB Bandwidth =-8.07870491132E-09
Amplitude of tone = 1.51325861755E-08
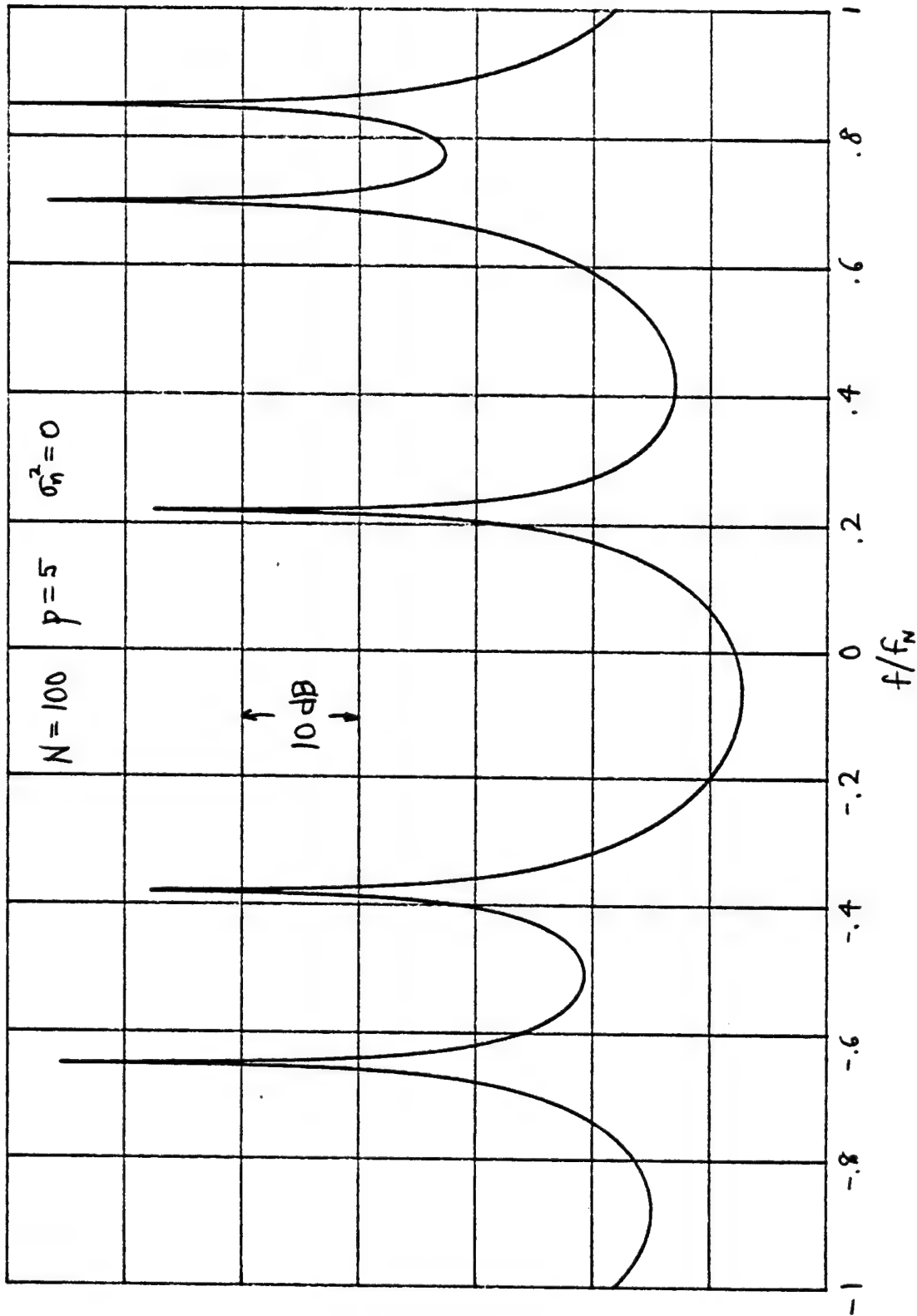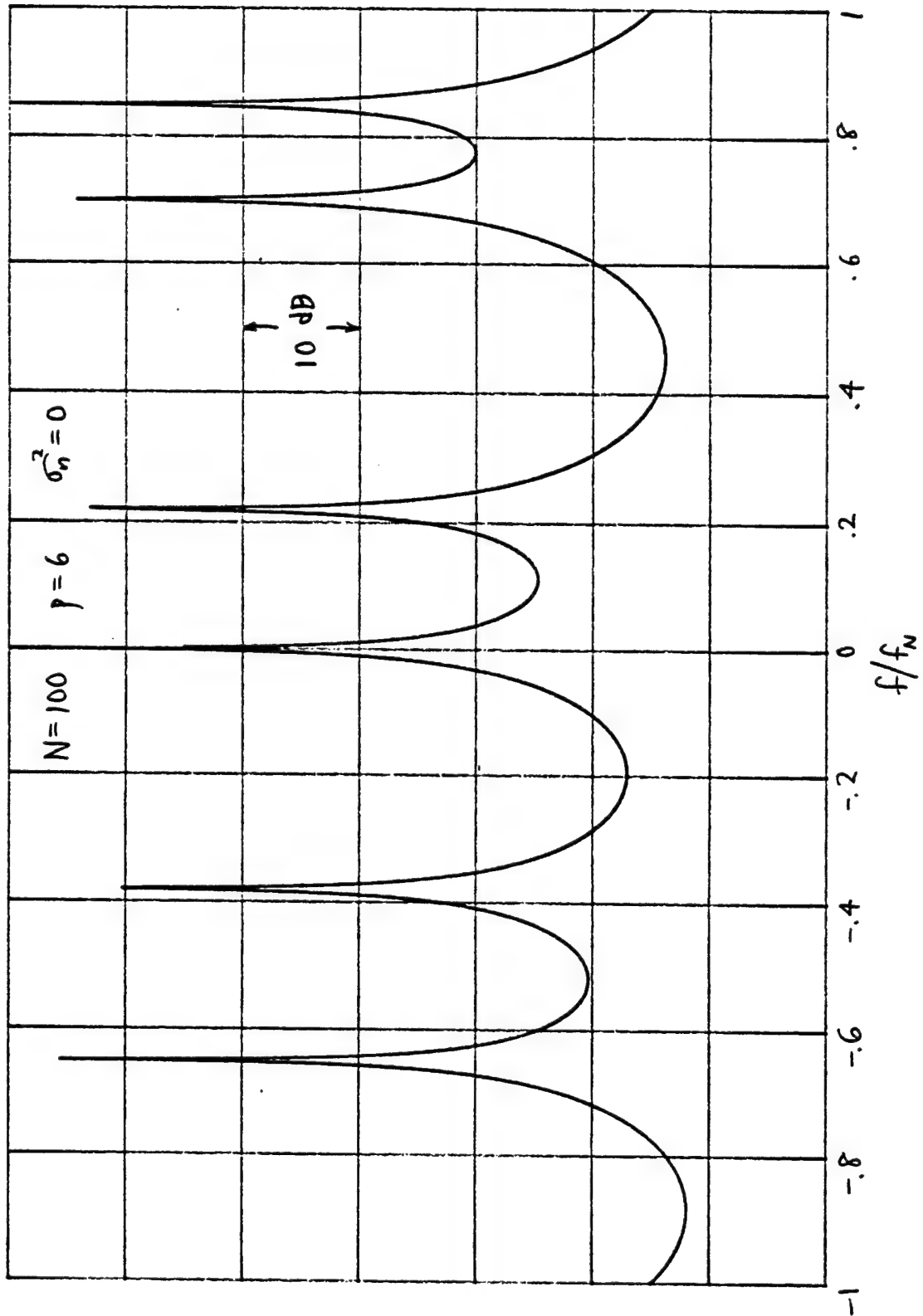
Table B-2. Sample Mean Subtracted; p = 6

Figure B-2. Sample Mean Subtracted; p = 6

LINEAR PREDICTIVE SPECTRAL ANALYSIS FOR COMPLEX DATA.
FORWARD AND BACKWARD AVERAGING. MARPLE ALGORITHM, 5 DEC 79.
FILTER WEIGHTS; SPECTRUM; POLE LOCATIONS AND POWERS.
NUMBER OF COMPLEX DATA POINTS = 100
MAXIMUM ORDER OF FILTER = 5

MEAN OF DATA = -2.00000000267E-02 -3.72722031951E-03 *not subtracted*
VARIANCE OF DATA = 4.87999999992

STATUS OF STOPPING CRITERION = 4
PREDICTION-ERROR POWER =-3.44715489882E-11
OPTIMUM ORDER OF FILTER = 5
PREDICTION-FILTER WEIGHTS:
-.794144480748   .079648473805
-.737462942076   -.263405789893
-.312813565611   .717901019815
-.6016905446   .524383279876
-.684547105931   .728968627434

VARIANCE FROM GRAPH =-1.03588935768E-08

LOCATIONS OF POLES: REAL,IMAG,MAG,ARG/PI

-.453990499742   -.89100652419   1   -.65
Power content of pole = 0   3 dB Bandwidth = 0
Amplitude of tone = .970168678098

 .368124552691   -.929776485885   1   -.379999999997
Power content of pole = 0   3 dB Bandwidth = 0
Amplitude of tone = .980342883582

 .770513242777   .63742398975   1   .219999999999
Power content of pole = 0   3 dB Bandwidth = 0
Amplitude of tone = .980010321793

-.587785252291   .809016994384   1   .7
Power content of pole = 0   3 dB Bandwidth = 0
Amplitude of tone = .931164116992

-.89100652419   .453990499752   1   .85
Power content of pole = 0   3 dB Bandwidth = 0
Amplitude of tone = .971017604263

Table B-3. Sample Mean Not Subtracted; p = 5
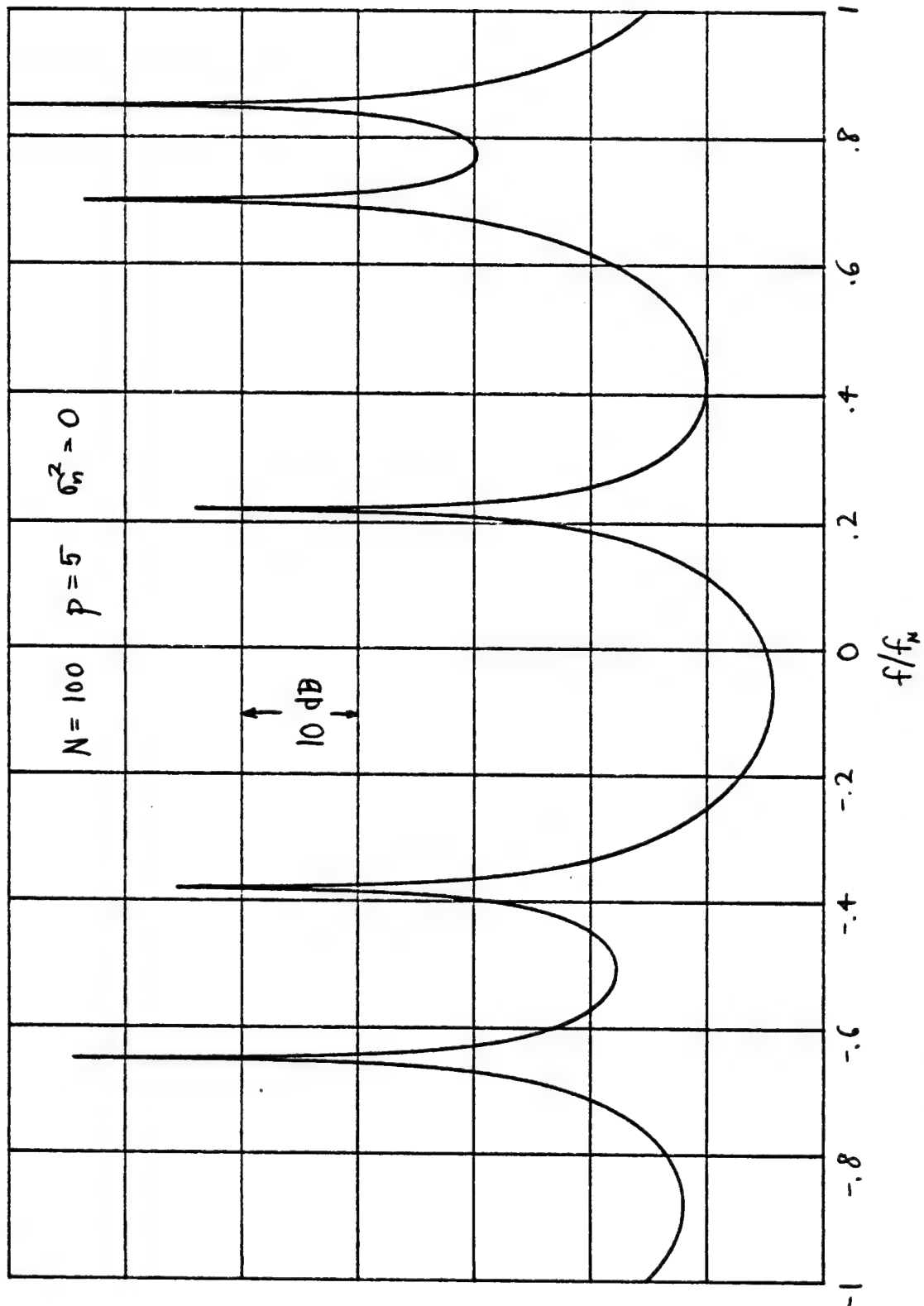
Figure B-3. Sample Mean Not Subtracted; $p = 5$

Graph annotations:
$N = 100$ $p = 5$ $\sigma_n^2 = 0$
10 dB
f/f_N

APPENDIX C. DETECTABILITY CRITERION

Suppose a received waveform $x(t)$ is characterized as follows:

$$x(t) = \begin{cases} s(t) + n(t), & H_1 \\ n(t), & H_0 \end{cases}, \tag{C-1}$$

where $s(t)$ is a deterministic signal waveform and $n(t)$ is a stationary noise process with spectrum $G_n(f)$. Let us process $x(t)$ linearly according to correlation operation

$$z = \int dt\, w(t) \times (t), \tag{C-2}$$

where weighting $w(t)$ is to be selected to maximize the deflection of output random variable z. Letting m and σ^2 be the mean and variance of z, we define deflection

$$d^2 \equiv \frac{(m_{s+n} - m_n)^2}{\sigma_n^2} = \frac{\left[\int df\, W(f)\, S^*(f)\right]^2}{\int df\, |W(f)|^2 G_n(f)} \tag{C-3}$$

for processor (C-2). The optimum weighting is found to be

$$W_o(f) = \frac{S'(f)}{G_n(f)}, \tag{C-4}$$

with corresponding maximum value

$$d_o^2 = \int df\, \frac{|S(f)|^2}{G_n(f)}. \tag{C-5}$$

Now suppose that signal $s(t)$ is narrowband, so much so that the bandwidth of $|S(f)|^2$ is narrower that the finest detail of $G_n(f)$ at the signal center frequency f_s. Then (C-5) becomes

$$d_o^2 \cong \frac{1}{G_n(f_s)} \int df\, |S(f)|^2 = \frac{E}{G_n(f_s)}, \tag{C-6}$$

where E is the received signal energy; this result is typical in white noise backgrounds. This latter quantity is a "local" measure of signal-to-noise ratio at f_s, and is the governing statistic for detectability. Values of (C-6) greater

than 10 are typically needed for good detection and false alarm probabilities.

Let us now consider a sampled process, with time increment Δ, and $f_N = (2\Delta)^{-1}$. Then we can let

$$G_n(f) = G_n(0)\, \mathcal{S}(f/f_N) \quad \text{for} \ |f| < f_N, \tag{C-7}$$

where $\mathcal{S}(u)$ is a shape function defined over $|u| < 1$, with value 1 at $u = 0$. Then noise power

$$\sigma_n^2 = \int_{-f_N}^{f_N} df\, G_n(f) = G_n(0)\, f_N \int_{-1}^{1} du\, \mathcal{S}(u), \tag{C-8}$$

giving

$$G_n(f) = \sigma_n^2\, 2\Delta\, \frac{\mathcal{S}(f/f_N)}{\int_{-1}^{1} du\, \mathcal{S}(u)} \quad \text{for} \ |f| < f_N, \tag{C-9}$$

in terms of σ_n^2 and the shape function.

If our signal consists of a pure tone of frequency f_1 and amplitude A_1, and duration N samples, then

$$E = \frac{A_1^2}{2}\Delta N, \tag{C-10}$$

and (C-6) yields

$$d_o^2 = \frac{A_1^2/2}{\sigma_n^2} N\, \frac{\int_0^1 du\, \mathcal{S}(u)}{\mathcal{S}(f_1/f_N)}. \tag{C-11}$$

The leading term in (C-11) is the SNR of this signal tone, referred to the total noise in the band $(-f_N, f_N)$. The number of samples available, N, enters linearly into this result. And the last term depends on the shape of the noise spectrum.

The noise example we will consider is that depicted in figure 14, namely

$$n_k = 3\alpha\, n_{k-1} - 3\alpha^2\, n_{k-2} + \alpha^3\, n_{k-3} + W_k, \tag{C-12}$$

where W_k is white noise with variance σ_w^2, and

$$\alpha = 0.7. \tag{C-13}$$

We find, for example (C-12),

$$G_n(f) = \frac{\Delta \sigma_w^2}{\left| 1 - \alpha \exp\left(-i\pi f/f_N\right)\right|^6} \quad, \quad |f| < f_N$$

$$\mathcal{S}(u) = \frac{(1-\alpha)^6}{\left| 1 - \alpha \exp\left(-i\pi u\right)\right|^6} \quad, \quad |u| < 1$$

$$\mathcal{S}(0) = 1, \quad \mathcal{S}(1) = \frac{(1-\alpha)^6}{(1+\alpha)^6} \quad \left(= -45.2 \text{ dB} \quad \text{for} \quad \alpha = 0.7\right)$$

$$\int_0^1 du \, \mathcal{S}(u) = \frac{(1-\alpha)(1+4\alpha^2+\alpha^4)}{(1+\alpha)^5} \quad \left(= .067615 \quad \text{for} \quad \alpha = 0.7\right)$$

$$\sigma_n^2 = \sigma_w^2 \frac{1+4\alpha^2+\alpha^4}{(1-\alpha^2)^5} \quad \left(= 92.75 \sigma_w^2 \quad \text{for} \quad \alpha = 0.7\right) \tag{C-14}$$

Substitution in (C-11) yields

$$d_0^2 = \frac{A_1^2/2}{\sigma_n^2} N \frac{1+4\alpha^2+\alpha^4}{(1-\alpha^2)^5} \left| 1 - \alpha \exp\left(-i\pi f_1/f_N\right)\right|^6 \tag{C-15}$$

$$= \frac{A_1^2/2}{\sigma_w^2} N \left| 1 - \alpha \exp\left(-i\pi f_1/f_N\right)\right|^6. \tag{C-16}$$

Equation (C-15) is evaluated in table C-1 for the parameters of figure 22. It will be observed that values of d_0^2 less than approximately 15 correspond to tones that are difficult to detect in figure 22, whereas values of d_0^2 greater than 15 correspond to the detected tones in figure 22. Thus the linear predictive

technique yields not only the spectral estimate of the process under investigation, but also detects tones at local SNRs only a couple of dB poorer than an optimum processor. The quantitative measure in (C-6) is a very useful parameter for quickly ascertaining the detectability of tones in colored noise.

f_1/f_N	$\dfrac{A_1^2/2}{\sigma_n^2}(dB)$	d_o^2
.07	-10	17.6
.15	-20	13.2
.35	-30	57.9
.375	-30	80.6
.45	-30	190.4
.65	-40	89.1
.75	-50	14.1
.95	-50	22.0

Table C-1.   Deflections for Figure 22; N = 1000, $\alpha = 0.7$

REFERENCES

1. J. Makhoul, "Linear Prediction: A Tutorial Review", <u>Proc. IEEE</u>, vol. 63, no. 4, April 1975, pages 561-580

2. T.J. Ulrych and T.N. Bishop, "Maximum Entropy Spectral Analysis and Auto-regressive Decomposition", <u>Reviews of Geophysics and Space Physics</u>, vol. 13, no. 1, Feburary 1975, pages 183-200

3. A.H. Nuttall, "Spectral Analysis of a Univariate Process with Bad Data Points, via Maximum Entropy and Linear Predictive Techniques", NUSC Technical Report 5303, 26 March 1976

4. J.P. Burg, "A New Analysis Technique for Time Series Data", NATO Advanced Study Institute on Signal Processing, Enchede, Netherlands, vol. 1, August 1968

5. S.L. Marple, "A New Autogregressive Spectrum Analysis Algorithm", submitted to <u>IEEE Trans. on Acoustics, Speech, and Signal Processing</u>, August 1979

6. S. Kay and S.L. Marple, "Sources of and Remedies for Spectral Line Splitting in Autoregressive Spectrum Analysis", <u>Proc. IEEE, ICASSP</u>, 1979, pages 151-154

7. R.T. Lacoss, "Data Adaptive Spectral Analysis Methods", Geophysics, vol. 36, no. 4, August 1971, pages 661-675

8. O.L. Frost, "Power-Spectrum Estimation", NATO Advanced Study Institute on Signal Processing, with Emphasis on Underwater Acoustics, Portovenere, Italy, 30 Aug.- 11 Sept.1976. Also in Aspects of Signal Processing. Part I, G. Tacconi, editor, D. Reidel Publishing Co., Boston, 1977.

9. S.L. Marple, "Conventional Fourier, Autoregressive, and Special ARMA Methods of Spectrum Analysis", Engineer's Degree Thesis, Stanford Univ., Stanford, Calif., 3 Jan. 1977.

APPLICATION OF LINEAR PREDICTIVE SPECTRAL ANALYSIS
TO MULTIPLE TONES IN NOISE
A.H. Nuttall
Special Projects Dept.
Advanced Systems Technology Division
TM No. 791218
12 December 1979
JO #A75205
UNCLASSIFIED

DISTRIBUTION LIST

EXTERNAL

NAVMAT (J. Probus, 08T1)

INTERNAL

A.H. Nuttall, 313
A. Ellinthorpe, 3103
B. Buehler, 3103
H. Freese, 3103
P. Stocklin
P.G. Cable, 313
P. Abraham, 313
C. Arnold, 313
C. Carter, 313
M. Lackoff, 313
A. Quazi, 313
D. Viccione, 101
J. Ferrie, 317
A. Filippini, 333
F. DiNapoli, 312
R. Johnson, 441
J. Sikorski, 441
A. Markowitz, 323
C. Nawrocki, 3372
N. Owsley, 317
R. Kneipfer, 317
J. Fay, 317
H. Newman, 317
J. Wolcin, 317
R. Mellen, 313
T. McAndrew, 317
S. Dzerovych, 317
W. Roderick, 312
P. Herstein, 312
C. Becker, 312
R. Radlinski, 313
W. Fischer, 317
J. Ianniello, 317
R.H. Bernier, 721
7213 (3)
7223
72254 (10)

EXTERNAL: 1
INTERNAL: 48
    TOTAL 49